PLANT-STAND COUNT AND WEED IDENTIFICATION MAPPING USING UNMANNED AERIAL VEHICLE IMAGES

A Thesis
Submitted to the Graduate Faculty
of the
North Dakota State University
of Agriculture and Applied Science

By

Dharani Suresh Babu

In Partial Fulfillment of the Requirements
for the Degree of
MASTER OF SCIENCE

Major Program:
Environmental and Conservation Sciences

November 2018

Fargo, North Dakota

NORTH DAKOTA STATE UNIVERSITY

Graduate School

Title

PLANT-STAND COUNT AND WEED IDENTIFICATION MAPPING USING UNMANNED AERIAL VEHICLE IMAGES

By

Dharani Suresh Babu

The supervisory committee certifies that this thesis complies with North Dakota State University's regulations and meets the accepted standards for the degree of

MASTER OF SCIENCE

SUPERVISORY COMMITTEE:

Dr. Igathinathane Cannayen
Chair

Dr. Halis Simsek

Dr. Peter Oduor

Approved:

November 15, 2018
Date

Dr. Sreekala Bajwa
Department Chair

ABSTRACT

Modern agriculture encounters several challenges these days. There is a vital need for spatial data about plant and weed distributions. Obtaining accurate knowledge of the plants and weeds distribution in the field with manual methods are time-consuming. In this research, image processing programs were developed from the unmanned aerial vehicle (UAV) digital images to obtain the plant-stand count and weed identification and mapping in the field. Algorithms using pixel-march with search-hands criterion for the plant-stand count and shape-based features for weed identification were developed. Results were found to be accurate in the cropped UAV stitched images (>99 %) in manual image-based validation. User-friendly message windows, labeled images, textual results, and distribution maps were produced as outputs. The outcomes of this study will enable farmers to determine the plant and weed distributions in the field and will be helpful in deploying precision agriculture measures.

ACKNOWLEDGEMENTS

I would like to take this opportunity to express my sincere gratitude and respect to all those who made this thesis possible. First and foremost, I take pride and I would like to express my gratitude and respect to my advisor, Dr. Igathinathane Cannayen, Associate Professor, Agricultural and Biosystems Engineering (ABEN). His quality of being extremely patience and systematic way of approaching research is remarkable and he implements these while dealing with students as well. Students working under him were trained to be the best persons both professionally and personally. I would always strongly suggest any students work under him, if they get an opportunity. Recently, I came across an article written by Ms. Gundula Bosch, Director of R3 Graduate Science Initiative at Johns Hopkins Bloomberg School of Public Health in Baltimore, Maryland who said, “Train Ph.D. students to be thinkers not just specialists”. Dr. Cannayen train students with dedication and make them to think and become good researchers. I am honored working with Dr. Cannayen and waiting for my next opportunity to work with him.

I take honor and would like to thank Dr. Joao Paulo Flores, Precision Agriculture Specialist, Carrington Research Extension Center, NDSU, the other principal investigator of this funded project. The funding provided by the investigators Drs. Flores and Cannayen made me feel blessed, and without which it wouldn’t have been possible for me to come from India to the United States to pursue my MS program in Environmental and Conservation Sciences (ECS). I am humbled and thankful for this funding and support throughout the study.

I have great pleasure in acknowledging my gratitude to my supervisory committee members, Dr. Halis Simsek, and Dr. Peter Oduor for their valuable time, guidance, suggestions, and encouragement during this research. My heartfelt thanks to Dr. Craig Stockwell, Professor and Director of Environmental and Conservation Sciences graduate program, NDSU for extending his support by providing me an ECS ambassador assistantship during my early semesters at the university. It was indeed a great pleasure working under them. My sincere thanks to Dr. Sreekala Bajwa, Professor and Chair, ABEN, for encouraging me to explore different fields and for extending moral support.

This work was supported by the funds of AES Precision Agriculture (Fund numbers: FARG080004), and in part by the USDA, NIFA, NDSU Hatch Projects (ND01472 and ND01481 with accession numbers: 229896 and 1014700, respectively). These funding supports are thankfully acknowledged. Research and office facilities provided by the Northern Great Plains Research Laboratory (NGPRL), USDA-ARS, Mandan, ND and the excellent support extended by the NGPRL staff are also greatly appreciated.

Special thanks to Mr. Sunoj Shajahan, Ph.D. candidate, Ms. Subhashree N. Srinivasagan, Ph.D. student, Dr. Saravanan Sivarajan, Dr. Vidhya Kumar, Mr. Vidhya Shankar, Mr. Manu, Mr. Sunil and their family for their friendship and moral support.
I would like to thank Ms. Bonnie Cooper, NDSU Chapter of Golden Key International Honor Society, for proof-reading and providing valuable review comments in my thesis. I would also like to extend my thanks to Dr. Vincent Vadez, Dr. Jana Kholova, Dr. Jyostna Mura Devi, Scientists at ICRISAT and to TNAU, my bachelor's university, professors, who had been encouraging me constantly.

Finally, I would like to thank all the staff of ABEN, NDSU, and friends who have been very warm and helpful, supportive and encouraging, and any of this would not have been possible without them. I would like to thank God Almighty for giving me the strength, knowledge, ability, and opportunity to undertake this research study and to complete it satisfactorily.

DEDICATION

To my father, Mr. Suresh Babu Munusamy; mother, Mrs. Eswari Suresh Babu; brother, Mr. Dayanidi Suresh Babu; and KNM & Sons and PCP & Groups family. Always I owe and look upon a great eminent scientist Dr. A.P.J. Abdul Kalam as my role model in my life.

TABLE OF CONTENTS

LIST OF TABLES

LIST OF FIGURES

LIST OF ABBREVIATIONS

AUVSI	Association for Unmanned Vehicle Systems International
CIVE	Color Index of Vegetation Extraction
CPU	Central Processing Unit
CREC	Carrington Research Extension Center
ExG	Excess Green Index
GEM	Genotype × Environment × Management
GIS	Geographic Information System
GPS	Global Positioning System
ICT	Information and Communication Technology
IDE	Integrated Development Environment
LAI	Leaf Area Index
LiDAR	Light Detection And Ranging
NDI	Normalized Difference Index
NDVI	Normalized Difference Vegetation Index
NIR	Near-Infrared
RGB	Red Green Blue
SSWM	Site-Specific Weed Management
UAS	Unmanned Aerial System
UAV	Unmanned Aerial Vehicle
UTM	Universal Transverse Mercator
VEG	Vegetative Index
VRA	Variable Rate Application

LIST OF APPENDIX FIGURES

1. GENERAL INTRODUCTION

Agriculture should and always embraced new technologies to maximize the efficiency and to minimize the inputs in order to move towards sustainability. The vital need for spatial data about plant and weed distributions to explore genotype × environment × management (GEM) interactions was understood and being explored. Recently, with modern precision agriculture, there is a growing interest for using modern technology, such as the application of an unmanned aerial vehicle (UAV) or an unmanned aerial system (UAS) along with image processing. The UAVs, which are popularly called drones, are automated, pilotless aircraft which can be remotely controlled by using flight plans that can be set with programming or through dynamic systems based on a global positioning system (GPS). UAVs have many benefits and have been used in many industries, such as defense, construction, surveying, digital surface modeling and mapping, surveillance, archaeology, and several other fields (Nex & Remondino, 2014). In general, UAV applications in agriculture are new, and they are open to several research possibilities and the development of practical methods.

Traditionally, agricultural field management was performed as a "blanket" application or as a "uniform" application of fertilizers, herbicides, fungicides, and irrigation for the crops being grown. This traditional application was not very efficient, and it led to wasted resources. In recent years, the development of GPS and geographic information systems (GIS) led to the advancement of precision agriculture for site-specific field management. The UAV applications for the fields help farmers/producers to overcome the

shortcomings of uniform applications in an efficient way by enabling variable-rate zone application for the nutrients, plant-protection chemicals, soil management, or crop-stress management based on the local field requirements (Rudd et al., 2017).

In precision agriculture, manned aircraft vehicles can be used for image capturing or for spraying chemicals over the large fields; however, UAVs not widespread and efficient for the most prevalent medium and smaller fields. UAVs fly at a low altitude and capture high-resolution images that are suitable for further image processing. The UAVs' endurance level is based on their batteries, which is their power source; hence UAVs are suitable for smaller field areas (Lu et al., 2015). Thus, UAVs are developed as cost-effective alternatives, and agricultural field operations can benefit from using UAVs for a shorter period (Huang et al., 2013). UAVs have been created with different models, configurations, sizes, and shapes for various applications. UAVs were used for crop dusting in agriculture fields during 1980s, and eventually, the UAV applications with fields increased rapidly for aerial photography and crop imaging over the agricultural fields for precision agriculture management.

Direct-contact sensors that measure crop- and soil-related parameters are available or can be developed for various agriculture applications. However, contactless and remotely operated sensors use indirect measurements (such as color, temperature, and spectral wavelengths) that can be integrated with UAVs and have a wider coverage area. By using UAV sensors and measuring indirect variables, the plant's phenological and physiological characteristics can be correlated and studied. For instance, leaf color is helpful to identify the crop's growth stages, diseases, and pest attacks. In this regard, a normalized difference vegetation index (NDVI), which is a graphical color representation of

vegetation ranging between -1.0 to $+1.0$ (Primicerio et al., 2012), can be derived from the component color channels (R, G, B, and NIR) of the digital color images that were obtained from the UAV mounted cameras through image processing.

Plant populations, in general, can influence the yield and can cause reduction in crop yield. In corn, it was found that yield was maximized with particular plant populations depending upon nutrient availability (Duncan, 1958). Many researchers examined the relationships between the corn's population density and yield. The two field variables that have a larger effect on the final yield are plant-population density (Willey & Heath, 1969) and inter-plant spacing (Nafziger, 1996). Seed germination, planter-seed placement, and plant death were the three main causes of variability for plant spacing (Nielsen, 2001). Manual stand counts are laborious, are not feasible for large field areas, and are susceptible to human error. Challenges involved with stand counting include plant-row identification, plant-row straightness (linear or curvilinear), plant-size variation (projected area), and the plants' spatial variation which is represented as "doubles" ($< \frac{1}{2}$ ideal spacing) and "skips" ($> \frac{1}{2}$ ideal spacing). An automated, non-subjective plant-counting system would provide a method to quantify plants objectively, precisely, and quickly, which are always desirable.

It is now understood that a blanket, or uniform, application of herbicides (or pesticides) to the crops is inefficient and not profitable for the farmers/producers. Weeds are found randomly in the agricultural fields, either as large/small patches or individually, based on the weed variety. It is inefficient to apply chemicals as a uniform application to the entire field, and such applications are harmful to the environment, too. Several predominant weeds were identified in North Dakota (Zollinger et al., 2006), and targeted spraying the herbicides, rather than applying them uniformly to the field, is the most

efficient approach. For such precision agriculture applications, the most important step is to identify and to quantify the weeds or diseased plants; then, the weeds are mapped in the field. UAVs can be utilized to capture images that are processed in order to identify and to map the weeds (Pena et al., 2013).

With suitable image processing, applications such as plant-stand count as well as weed identification and mapping are possible with the images from the UAV cameras or other input devices. Because digital images (visual or spectral) can be represented by an array of numbers, inspecting and manipulating the numbers based on user-designed algorithms make image processing possible in order to address specific challenges and to develop user-specific products.

With this background, this thesis focused on developing plant-stand counting and weed-identification algorithms using the UAVs' visual images while employing ImageJ software. ImageJ is an open-source, free, Java-based programing system that allows people to develop user-coded plugins (programs developed by users) to solve the image-processing problem that represents the chosen practical applications. The developed plugins utilize the digital images as inputs, which will run in ImageJ and then produce the processed images and/or textual outputs.

1.1. Statement of Objectives

The major objectives of this research work are:

1. To review the applications of UAVs for crop growth and health monitoring.
2. To develop a digital image processing program for counting plants, identifying plant rows, quantifying "skips" and "doubles" in a straight and curvilinear plant rows from UAV images.

3. To develop a digital image processing program for identifying different types of weeds in the agricultural fields from UAV images.

1.2. Thesis Organization

The thesis consists of chapters such as (i) general introduction, and the study's objective is presented in the form of three (ii, iii, and iv) peer-reviewed journal articles, (v) general conclusions, combined references, and an appendix. A commonly presented "Review of Literature" chapter was replaced by the 3rd chapter in the form of a paper entitled "A review of unmanned aerial vehicles application for crop-growth and health monitoring", which also presents the similar material that is expected from the traditional Review of Literature chapter. Each of the chapters that are presented in the form of research paper is complete with its own introduction with supporting review of literature, materials and methods, results and discussion, and conclusions.

The chapters in the form of journal articles. Paper 1 entitled: "A review of unmanned aerial vehicles application for crop-growth and health monitoring" compiled the various research on UAV applications as a review article in the field of crop growth and health (Objective 1); Paper 2 entitled: "Automatic plant-stand count and spatial distribution using unmanned aerial vehicle digital images" described the development of an ImageJ plugin that analyzed the digital images of corn fields for plants row identification, stand count along rows, and plant distribution (skips and doubles) in the field; and Paper 3 entitled: "Shape-based weed identification and mapping using low-altitude unmanned aerial vehicle images" described the development of an image processing plugin that identified and mapped the two most common weeds of North Dakota from the corn field based on geometrical features of the image objects (Objective 3).

The “General conclusions and suggestions for future work” chapter summarized the results derived from the papers (1–3) in the section “General Conclusions”, and also presented was the “Suggestions for Future Work.” The “References” listing of the chapters was collected and presented as a separate final chapter. Appendices A and B presented some of the common weed species and some portions of the developed ImageJ plugin code.

2. A REVIEW OF UNMANNED AERIAL VEHICLES APPLICATION FOR CROP-GROWTH AND HEALTH MONITORING

2.1. Abstract

The UAV technologies significantly contribute to precision agriculture for optimizing the available agricultural resources and could play a large role in sustainable agriculture. Satellite images may not have the high resolution, which is necessary for precision agriculture applications with small field sizes. UAV technologies could address this issue by assisting with gathering information at the required frequency for continuous plant monitoring. This technology produces satisfactory resolution crop images, and with effective data analysis, useful information can be extracted, which could provide a decision support system for agriculture. There have been several recent studies about the application of UAVs with agriculture, but surprisingly, research about knowledge extraction using the images and data analysis from the images is relatively scant. Therefore, this review paper's objective was to focus on the use of UAV technologies in agriculture along with the exploration of data analytics using the captured images. The review synthesizes the available results about UAV technology applications in agriculture, identifies research gaps, and provides recommendations. The outputs are helpful to farmers, producers, UAV operators, and researchers for making informed decisions when selecting and employing UAV technologies to increase the effectiveness of mechanical agriculture and to perform future research.

2.2. Introduction

The UAV technology has existed for a few decades, but its potential use in agriculture was realized recently by capturing sequential images in order to gain scientific information and field scouting. In the next few years, the market value for UAVs in agriculture will increase by 80 % (4Deloitte, The Aerospace and Defense Industry in the U.S., A financial and economic impact study, March, 2012, written in Association for Unmanned Vehicle Systems International [AUVSI] economic report). This percentage signifies the reputation of UAV applications in agriculture. With the invention of novel and effective technologies, UAVs have the potential in the agricultural industry to deliver the site-specific farming management. When realizing the importance of drone applications in many industries, including agriculture, there are many openings for business opportunities, and increased investments are in this field.

Agricultural production can be significantly affected due to the influence of the surrounding environment in terms of soil, water, and weather conditions. Swain et al. (2007) suggested that drone technology provides an important characteristic: a solution, which is extremely sensitive to both environmental conditions and management practices. It is, thus, very important for the farmer to know where a problem exists in the field in a timely manner so that he/she can modify agricultural practices or solve the existing issue. Therefore, any techniques which increase agricultural productivity while helping to control the environmental effect will certainly help society. There is an example of integrating this technology with sensors which can identify the field variability, such as variable rate application (VRA) technology, along with combining grain-yield monitors and a GPS to

help with issues that arise due to agricultural management practices regarding irrigation management and yield estimation, respectively (Stafford, 2000).

As a result, precision agriculture provides a realistic means for optimizing resources, potentially reducing the effect of harmful compounds that affect the soil and atmosphere, and precision agriculture helps to greatly reduce the excess use of fertilizers, pesticides, fungicides, and herbicide applications. Despite having all these advantages, UAV application in agriculture had been also few other issues which need to be addressed, such as the lack of an efficient decision-support system, insufficient accuracy with temporal variation, and environmental auditing (Mcbratney et al., 2007).

The purpose of this review is to provide insight by defining the application of the UAVs remote sensing in precision agriculture by exploring the current uses and limitations of drones in environmental monitoring and precision agriculture, including platforms such as the UAVs data-processing issues, cost-effective images, and farmers participation (Quilter, 1997).

2.3. Information and Communication Technology in Agriculture

Using technology for agriculture is one of the best solutions to meet the rapidly increasing population's larger food demand. Agricultural production needs to be 70 % higher in order to meet the food demand. To address this issue, information and communication technology (ICT) could play an important, practical role in precision agriculture and this has been explained well in Gartner's hype cycle, and (Fig. 2.1) explains this cycle in detail (Shi et al., 2016). Among the many existing ICT technologies, remote sensing is a prominent method of capturing aerial view images of agricultural farms for processing and analysis.

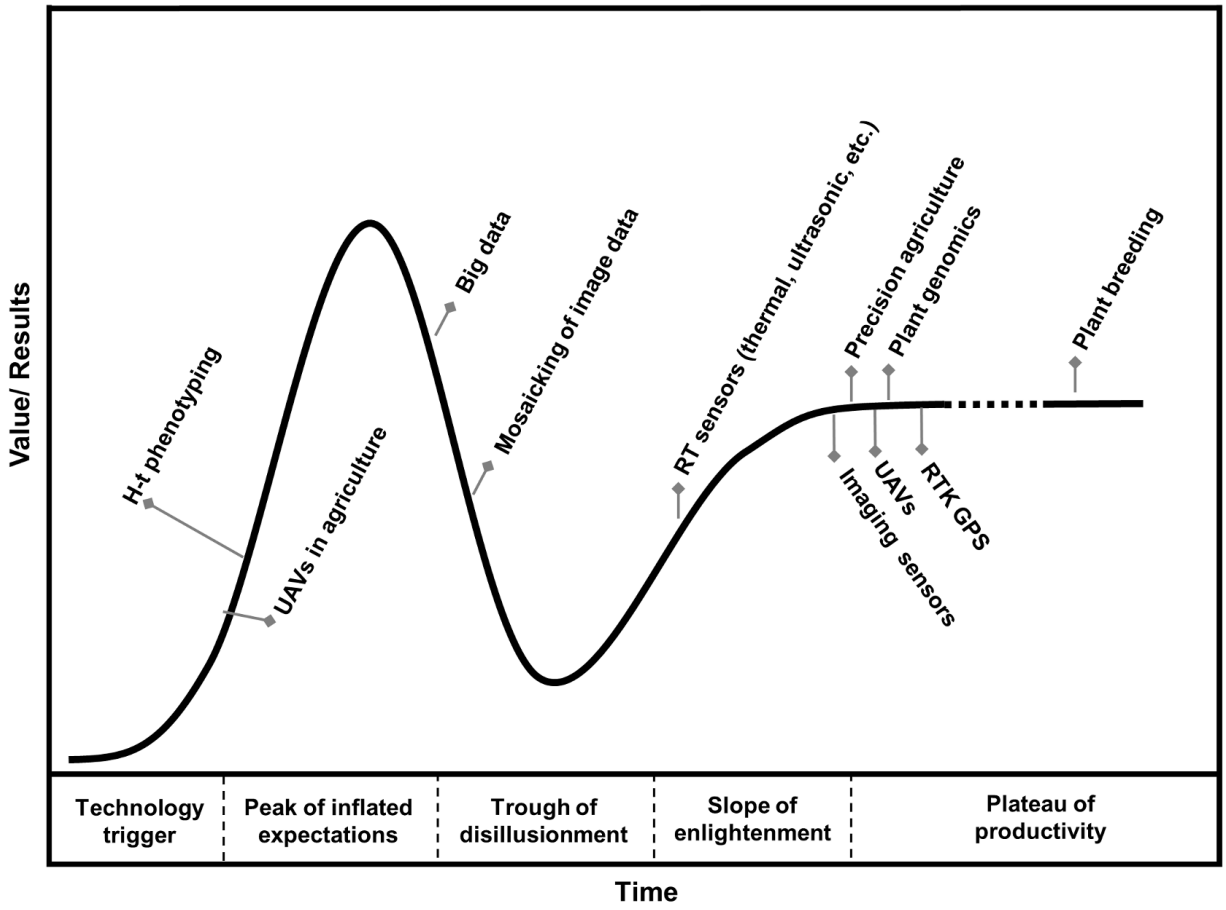

Figure 2.1. Gartner hype cycle — various development of technologies and integration of various multidisciplinary technologies (*Source*: Shi et al., (2016)).

2.3.1. Remote Sensing Technology

Remote sensing technology includes UAV/UAS and GPS that can be utilized to provide the optimum and precise amounts of water, fertilizers, and plant-protection chemicals. The VRA can be achieved by using this technology. Proper application of these technologies will increase crop production and will also support proper farm management, reducing the manual labor requirement (Abdullahi et al., 2015).

This technology can be considered as “smart farming”, which includes “big-data” applications and various stages of data management, such as image capturing, storage, transfer, transformation, analysis, and visualization. Also, the data need to be converted from raw images (data) to forms by preprocessing so that image-processing operations can be utilized to extract useful information.

2.4. Unmanned Aerial Vehicle Applications

In the early 1950s, precision agriculture was a popular management technique which created a revolution in the agriculture industry (Colwell et al., 1956). Crop scouting, also referred to as field scouting, is a historical method where farmers would monitor the land to find pests and weeds, to make a recommendation about applying inputs, and to make other management decisions. However, manual scouting is a very time-consuming task and relies heavily on random sampling, which has been observed to have many inaccuracies due to human error.

Recently, with the increased use of UAV applications for crop field management, many agricultural industries realized the technology’s potential use in precision agriculture to obtain high-resolution imagery, data, and information relative to existing methods, such as satellite imaging or manual crop scouting. These industries, along with collaboration from many profitable and non-profit organizations, started to provide timely solutions such a crop-scouting practices, for farmers. People realized that UAV technology would have a highly positive effect on the agricultural industry with planning and other strategies based on real-time data gathering and processing (Warren & Metternicht, 2005).

2.5. UAVs Flight Plan

In order to fly the drones, the pilot has to set the flight plans and wave points. The wave points are specified based on the fields' dimensions and orientation. The flight's height, speed, and amount of image overlap are specified as inputs. Based on these inputs, the drones fly and capture images, or record videos (Fig. 2.2). Usually, the UAV's onboard battery life determines the flight time and the size of the field that is captured. Distance-measuring equipment, such as ultrasonic echoing and lasers (including light-detection and ranging [LiDAR] lasers), helps the drones to modify the flight's altitude to avoid collisions.

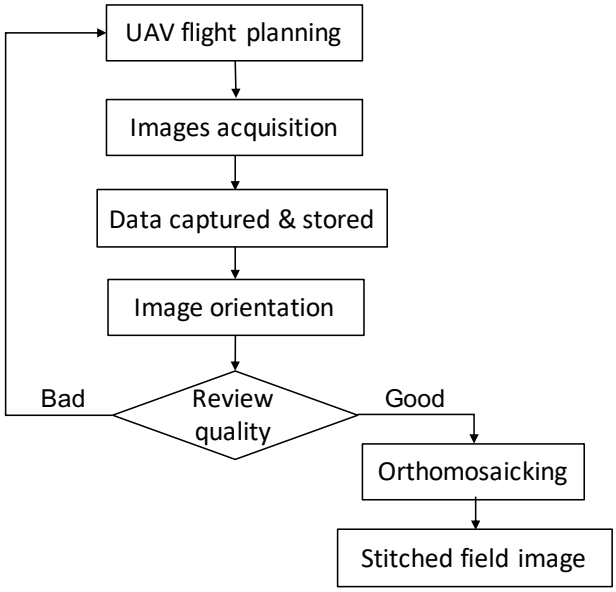

Figure 2.2. Process flow of UAV flight plan and image capture.

2.6. Types of UAVs

Based on the type and number of wings the drones have, the UAVs are classified into several types and are used for different purposes. The main two drone classifications are fixed-wing drones and rotary-wing drones.

2.6.1. Fixed Wing Drones

Fixed-wing drones are used for photogrammetric surveying, mapping, and other applications (Fig. 2.3). These purposes require drones to be stable for long-duration flights. With the elongated wings on either side of the drone's body, these UAVs' endurance level is high, so the drone can capture images of large fields on one charged battery. The UAVs can carry high-resolution cameras and are capable of capturing images with a finer resolution. For example, in a single flight, a fixed-wing drone at a flying altitude of 400 feet can capture images with a resolution of 2.9 cm for 540 acres of field area.

Figure 2.3. Fixed wing drone
(*Source*: `https://unmanned-aerial.com/senseflys-latest-fixed-wing-mapping-drone-is-here`).

2.6.2. Tricopters

Tricopters are drones with three propellers (Fig. 2.4). Although they are called tricopters, they have six rotors. There are three propellers and three motors on each side (top and bottom) of the tricopter drone. This tricopter is so efficient and cost-effective that it has overtaken the budgeted-drones market. The tricopters "hold" mode for altitude is a noticeable feature, which is accomplished by using barometers. Another noticeable

characteristic is taking off automatically and one-key operation for most of the tripcopters. These drones can only cover small field areas with multiple flights.

Figure 2.4. Tricopter
(*Source*: `https://newtechstore.eu/en/camera-drones/152-535-cheerson-cx-33c-tricopter-drone-with-10-mp-camera.html`).

2.6.3. Quadcopters

Drones with four propellers are called quadcopters (Fig. 2.5). The quadcopters are lifted by rotary wings or propellers instead of fixed wings. Two propellers rotate in a clockwise direction, and two propellers rotate in a counterclockwise direction. Thus, these drones can fly stably in the air. The propellers make these drones efficient and cost-effective for carrying heavy payloads when compared with a helicopter of the same size. The flight time is approximately 30 minutes, or it can be less with multiple flight runs. Quadcopters are the most commonly used drone type.

2.6.4. Hexacopters

Hexacopters have six propellers (Fig. 2.6). Propellers are located around the drone's body. A hexcopter is more powerful than tricopters and quadcopters because of its six

Figure 2.5. Quadcopter
(*Source*: `https://www.dji.com/phantom-4-pro`).

propellers and its ability to carry heavier payloads. The biggest advantage of a hexacopter is that, even when one propeller fails, the drone can continue flying by using the other five propellers, thus the drone will not prematurely crash during the flight. If two propellers fail, then the drone will not take off. Compared to a quadcopter, the hexacopter can fly at higher altitudes and at a faster rate. Compared to tricopters and quadcopters, the hexacopter is expensive; hence, it is generally used for commercial purposes. The flight duration can be up to 20 or 30 minutes, depending on the drone's payload.

2.6.5. Octocopters

Octocopters have eight propellers (Fig. 2.7). The octocopter is more powerful when compared to quadcopters and hexacopters. It can fly at higher altitudes and can carry heavier payloads. Because the octocopter has eight propellers, it will not hover in the air much. Eight blades offer the drone stability during flight. The octocopter records high-quality videos and captures high-resolution images because it can have heavier payloads. These copters can survive heavy winds and rain, and they will not crash even if

Figure 2.6. Hexacopter
(*Source*: `https://www.yuneec.com/en_GB/camera-drones/hexacopter.html`).

two or three propellers fail. Because of their high reliability, octocopters are suitable for the purpose of missions.

Figure 2.7. Octocopter
(*Source*: `https://www.dji.com/spreading-wings-s1000`).

2.7. Potential Uses of UAVs in Agriculture Research

UAV applications in agriculture have six major contributions: soil and field analysis, planting, crop spraying, crop monitoring, irrigation, and crop-health assessment. Many other applications are being explored for this UAV technology.

2.7.1. Soil and Field Analysis

Drones can be used at the beginning of the crop season to provide precise 3D maps for soil analysis, helping to plan seed-planting patterns. After sowing, this technology provides a drone-driven soil analysis, which greatly helps to manage irrigation and nitrogen applications. These management applications are crucial for the crops to grow and to produce a better yield (Corbane et al., 2012).

2.7.2. Planting

Start-ups have created drone-driven planting systems that are available to farmers; these systems help achieve the maximum growth rate and can reduce the initial planting costs by 85 %. These prospects are profitable for farmers and represent the technology's significant contribution. These planting systems include seed management and nutrient management (Wich et al., 2015).

2.7.3. Crop Spraying

Crop spraying with drones is an emerging technology. The drones scan the ground and apply the necessary amount of chemicals, such as fertilizers or pesticides, wherever required based on the programmed instructions. This method efficiently reduces the waste and the amount of chemicals that infiltrate into the groundwater, avoiding land and air pollution. It is estimated that this methodology is five times faster and more effective when compared with traditional methods (Zhu et al., 2010).

2.7.4. Crop Monitoring

One of the biggest hindrances for current agriculture is the large fields and low efficiency with crop monitoring. This problem was aggravated due to unpredictable climate conditions which put agriculture-management practices at risk. Previously, satellite imagery and remote-sensing platforms addressed these issues. The biggest drawback with satellite images was that the image capturing needs to be planned well in advance and cannot be done whenever necessary. Moreover, it is also expensive. The image quality was highly dependent on the weather conditions for the day of image capture (Honkavaara et al., 2013). However, drone technology was a boon in helping to solve this issue with sequential image capturing. Drones can obtain images whenever necessary, so the crop and its production can be monitored continuously. Sequential images from drones result in time-series animations, enabling better crop management.

2.7.5. Irrigation

The UAV technology utilizes different spectral cameras, including RGB, hyperspectral, multispectral, or thermal. By using different cameras to capture images, it is possible to identify which part of the field requires irrigation or needs improvement. During the crop's growing period, drones facilitate the calculation of vegetation indices which describe the plants' density and health. Thermal cameras show the heat signature and the amount of energy which the crop emits. These data are very useful for breeding specialists to develop drought-resistant varieties that are suitable for the world's semi-arid regions (Lambert & Faulkner, 1991).

2.7.6. Crop Health Assessment

It is always important to assess the crop's health and to spot bacterial or fungal infections in the crops. Plants reflect different amounts of green and near-infrared (NIR) wavelengths, and this can be captured as images by using visible and NIR cameras. The information can be utilized to track changes in the crop's health. Because this technology can provide prompt assessment, crops can be saved, and remedies can be given in a precise and timely manner. Furthermore, in the case of crop failure, the farmer can document losses more efficiently for insurance claims (Zhang & Kovacs, 2012).

2.8. UAV Image Analysis Indices in Agriculture Research

Color is an essential method which is used to discriminate plants from the soil background in the drone images. Several researchers have used color to differentiate plants from the soil. For example, color characteristics were utilized to distinguish green-colored plants from the soil (machine-vision technology) and to estimate the leaf area or leaf area index (LAI) (Meyer & Neto, 2008). Background extraction is done to remove the undesired region from the image, highlighting the crop by removing the soil background. The opposite thing can also be done, depending on the purpose. The most-commonly used visible-spectrum cameras are in RGB color space. Simply converting the RGB values into grayscale does not result in a good division because the plant and soil background pixels had similar grayscale values (Tian & Slaughter, 1998). In order to demonstrate good segmentation, the RGB space is often converted to different color spaces, such as Lab, HSV, or YUV. Several common green indexes are as follows.

2.8.1. Normalized Difference Index (NDI)

The NDI was defined by Woebbecke et al. (1993), and they introduced three different methods in RGB image to differentiate crop from the soil based on R, G, and B frequencies (e.g., [G-B], [G-R], and [G-R]/[G+R]). This index is functional to all pixels in the image and its values range between -1 and $+1$. But to display the image, these values must range between 0 and 255. Thus, the index was further modified by adding 1 to it and then multiplied by a factor of 128 to make available a grayscale image in the range of 0 to 255. Therefore, the formula of NDI is as follows:

$$\text{NDI} = 128 \times \left(\frac{G-R}{G+R} + 1 \right) \tag{2.1}$$

2.8.2. Color Index of Vegetation Extraction (CIVE)

The CIVE was defined by Kataoka et al. (2003) based on an experimental study in soybean and sugar beet fields. Crop growing stages can be projected using this method to separate crops from the soil background. The formula for CIVE is as follows:

$$\text{CIVE} = 0.441R - 0.811G + 0.385B + 18.78745 \tag{2.2}$$

This index has a better segmentation approach since it provides a greater importance to the green areas of the crop.

2.8.3. Vegetative Index (VEG)

The VEG is used to separate especially plants like cereal and weeds from soils (Hague et al., 2006). To perform the analysis using this index the images had been captured using a charge-coupled device camera. This index will convert the RGB scale

images into grayscale by using the following formula:

$$\text{VEG} = \frac{G}{R^a \times B^{(1-a)}} \tag{2.3}$$

where a is a constant value equal to 0.667. In addition, this index has a significant advantage of being robust to lighting change.

2.8.4. Excess Green Index (ExG)

The ExG was one of the several color vegetation indices studied by Woebbecke et al. (1995) using chromatic coordinates and modified the color in separating green plant from the soil background. The ExG color vegetation index is expressed as:

$$\text{ExG} = 2g - r - b \tag{2.4}$$

where r, g, and b are the chromatic coordinates are given by:

$$r = \frac{R^*}{R^* + G^* + B^*}; \quad g = \frac{G^*}{R^* + G^* + B^*}; \quad b = \frac{B^*}{R^* + G^* + B^*} \tag{2.5}$$

where R^*, G^*, and B^* are the normalized RGB values ranging from 0 to 1, and are computed as follows:

$$R^* = \frac{R}{R_{max}}; \quad G^* = \frac{G}{G_{max}}; \quad B^* = \frac{B}{B_{max}} \tag{2.6}$$

where R, G, and B are the actual pixel values from the images based on each channel and for a 24-bit color image.

Among selected color vegetation methods (Eqs. 2.1–2.6), it has been found that the ExG index (Eq. 2.6) was the best choice for differentiating plants from soil background

(Woebbecke et al., 1995). This is because ExG provided a clear distinction between plants and soil, and produced well-segmented binary images. Guerrero et al. (2012) studied the ExG index and found that it has been widely used and has performed very well in separating plants from non-plants.

2.9. UAVs Image Processing

The images captured using drones possess high radiometric similarity when compared to aircraft or satellite images due to the low altitude, which is utilized when capturing images (Lelong et al., 2008). This aspect is a noteworthy advantage of drone technology. However, drone-captured pictures have a lot of image-quality issues. For example, lightweight UAV systems hold the camera in a less stable position, resulting in poor spatial resolution (Lelong et al., 2008). Such artifacts also result in severe geometric alteration. This results in a technical problem for drone-captured images, such as blurred images which are not suitable for analysis purposes. To eliminate this adverse effect, image oversampling needs to be done, again resulting in a higher volume of data and leading to a difficult situation for handling large amount of data by storing the data and by processing them (Aber et al., 2009).

With a large number of images, image mosaicking is a necessary preprocessing step. There have been many successful cases using manual geometric correction to handle this issue (Vericat et al., 2009). This approach is not possible with larger areas that need to be monitored. This issue becomes the main concern that leads to UAV use with precision agriculture or site-specific management.

In order to address this issue, an effective automatic or semi-automatic photogrammetric approach was proposed (Laliberte & Rango, 2011). Although this

method is effective, geometric correction and ortho-rectification need to be done before the images can be combined because of the small swath area. Many other techniques, including manual geo-referencing using ground collected points, photo match, and automatic geo-referencing, also exist to address these issues (Xiang & Tian, 2011).

For practical purposes, the quality of the images collected by drones needs to be scrutinized so that the most suitable preprocessing methodology can be selected. There are many other issues, including bi-directional reflectance distribution, multiple-angle effects, and the effects from clouds as shadows, which need to be addressed during the preprocessing stage. Although some methods were proposed to deal with these effects (Lelong et al., 2008), different experiments require various and appropriate strategies to best address the issues in order to stimulate the next stage of information extraction. UAV-based remote sensing can be a good way to test these effects for other remote-sensing platforms (Aber et al., 2009).

In summary, problems with UAV image applications are generally fuzzy to the people who are utilizing applications with traditional aerial and satellite images. These problems include atmospheric correction, instrument calibration, line-shift correction, and frame mosaicking. For most applications, image-processing procedures must be automated so that the final image is delivered in an appropriate way. This has been observed to be of utmost importance for the UAVs' remote-sensing approach (Hardin & Jensen, 2011).

2.10. Algorithm Development

It is clear that applying UAVs for precision agriculture is still in the juvenile stage, leaving significant room for further development in terms of technology and data-extraction techniques. For now, the successful application of UAVs to monitor fields

reveals that using drones for site-specific management could be the next successful stage for remote-sensing applications, possibly contributing to increased agricultural production.

The preliminary examination was limited to individual plants which were observed against a soil background in controlled conditions. Vegetation and soil reflections will be different in the near-infrared region, which proved to be a successful approach for differentiating plants from the soil (Guyer et al., 1986). Plant diseases may manifest in different parts of the plant. There are methods to identify these diseases from the drone-captured images by exploring the visual indications for almost all the plant parts, such as roots (Smith & Dickson, 1991), kernels (Ahmad et al., 1999), fruits (Aleixos et al., 2002), stems(Corkidi et al., 2006), and leaves (López-García et al., 2010).

Methods such as artificial neural networks (Abdullah et al., 2007), thresholding (Sena Jr et al., 2003), dual-segmented regression analysis (Story et al., 2010), and others are becoming popular for plant counting, weed identification, crop-stress analysis, and the integration of vegetation indices. Yield estimation can be effectively performed using these different methods with the high-resolution, UAV-captured images.

2.11. Publications on UAV's Applications in Agriculture

The total number of peer-reviewed publications on UAV's applications in agriculture has also been reviewed and presented in Table 2.1. The review was performed in "Web of Science", a online scientific citation service. The search used the combination of keywords "UAV" & "...Application..." (listed in Table 2.1) with a filter of only journal articles. It is possible a single article can produce multiple hits if it addressed UAV and a combination of any of the considered applications (Table 2.1). However, the number publications shown is a good indicator of the volume of research carried out on UAVs application in agriculture.

Table 2.1. Number of peer-reviewed publications in major research areas of agriculture with UAV applications for 10 years ranging between 2007 to 2017.

S.No	Agriculture applications	Publication year	Number of publications
1	Irrigation	2014–2016	39
2	Yield estimation	2013–2016	275
3	Stand counting	2007 & 2014–17	66
4	Stress management	2009–2016	126
5	Weed management	2013–2017	44
6	Disease management	2013–2016	55
7	Pest management	2011–12 & 2015–17	26
8	Inventory management	2012–2017	53

The results showed the comparison between the total number of publications in main areas of agriculture with UAV applications in the past 10 years ranging between 2007 and 2017. It was found that a large number of studies was conducted in the yield estimation and crop stress management. So there is a great scope for the researchers to conduct research in other areas like irrigation, stand counting, field management (weed, disease, and pest), and inventory management.

2.12. Conclusion

The enhanced agreement between the drone's images and the ground's true data, the flexibility of image-acquisition times, and the cost-effectiveness should encourage researchers as well as the public and private sectors to consider drone technology as a key tool for precision agriculture endeavors. Fortunately, it is expected that, with the advanced drone technology and improved image-processing techniques, leading to a greater number of UAV studies based on remote sensing for agriculture application, there will be an appreciable benefit for precision agriculture and environmental monitoring. In this review, detailed information about different drone types, several drone-image capturing and

processing techniques, and various vegetation indices for agricultural field-image analysis were analyzed. Publication details about UAV applications in agriculture were given, which will help researchers/scientists to identify the research gaps and to develop research studies for the remaining issues. If UAV aviation regulations can be relaxed, research scientists may be more engaged with the farming community, and a greater adoption of UAVs for site-specific farming may occur.

3. AUTOMATIC PLANT-STAND COUNT AND SPATIAL DISTRIBUTION USING UNMANNED AERIAL VEHICLE DIGITAL IMAGES

3.1. Abstract

Determining the emergence and distribution of plants after they are seeded is an important measure for farmers and producers. It is challenging to accurately determine the plant count and distribution with the traditional approaches of manual observations and measurements. The manual method for plant surveys may be laborious, time-consuming, and result in undesirable disturbance to the plant ecosystems. The UAVs are increasingly used in precision agriculture, provide satisfactory levels of image features to estimate the plant's distribution and its vegetation types at a relatively low cost for small or large agriculture fields. In this research, corn, a row crop, was selected for testing and development. The digital, color images were obtained with a small-scale UAV to count the corn plants and to determine their distributions. Using an open-source ImageJ image-processing system, a robust plugin (program) was developed to count the plants and to determine the distance between plants, irrespective of the row's straightness. Techniques such as the pixel-march and search-hand criterion were introduced. The output also included the quantification of "skips" and "doubles" of plant emergence. Results were produced in 25–30 s, and plant counts obtained by using the developed algorithm were validated with manual, direct observations from the images; the plugin performance and

accuracy were found to be more than 99 %. Outputs were produced in various formats, such as message windows, field-prescription maps, textual forms, and tabular forms.

3.2. Introduction

In today's agriculture, the necessity of precision agriculture is on the rise. Through precision agriculture, the inputs can be optimized, and a higher yield can be achieved with an improved micro-level, spatial management of the field. More knowledge about agricultural inputs and outputs will help farmers/producers to manage their field efficiently; this knowledge can create more economic benefits. To achieve this, two main variables have a great influence with predicting the yield: knowing the plants' distribution as well as the plants' row and inter-spacing. The UAV technology has existed for a few decades, and its potential use in agriculture was recently realized by capturing sequential images in order to collect scientific data and for doing field scouting of the agricultural lands. In the next few years, the market value for UAVs in agriculture is going to increase by 80 %. This percentage signifies the reputation of UAV applications in agriculture. Agricultural production can be changed a lot due to the effect of the surrounding environment in terms of soil, water, and air quality. This drone technology provides a biological solution which is extremely sensitive to both environmental conditions and management practices (Swain et al., 2007). Any techniques which help to increase agricultural production also assist with controlling the harmful effects caused to the environment due to big machinery and large amounts of chemical applications for the agricultural field.

Corn plant populations can influence the yield. Corn yield is maximized at particular plant populations, depending upon nutrient availability (Duncan, 1958). Many researchers

have examined the relationships between the corn's population density and yield. These studies, which were conducted by different researchers, have found that the predictions had similar trends for yield maximization at particular plant population densities (Willey & Heath, 1969). Along with plant population studies, inter-plant distribution is also important for the effective utilization of available resources, such as nutrients and sunlight. If there is a missing plant in a row, the plants on either side of the missing plant only receive compensation for 47 % of reduced yield in a low-density agricultural field; for a high-density agricultural field, the compensation was 19 % of reduced field (Nafziger, 1996). The reasons for the plant-spacing difference could vary: plant death, poor seed germination, and improper seed placement. Weather and pest attacks could be other possible reasons for non-uniform plant distributions in the field (Nielsen, 2001). To achieve an effective variable-rate seeding, a farmer should have knowledge about his/her field's stand count for many years. Gaining this knowledge by manually counting the plants in the field is tedious and may have human errors (Bullock et al., 1998)).

To perform this analysis, an automated plant-counting system is necessary. This system provides a method to count plants quickly, objectively, and precisely. In addition, comparing early stage plant population measurements with the later-stage populations at harvest could be used to measure the plants' survival rate during the growing period. Then, the plant survival rates could be utilized to estimate the necessary population density for planting in order to achieve the desired population density. Many studies and technologies have been developed for population measurement, but most of them are utilized at harvest. Therefore, this study investigates machine-vision technology as a means of measuring the corn plant population at the early growth stage. Additionally, most studies have not

accounted for the plants which were placed/growing in a curvilinear pattern in the fields along with “skips” and “doubles” information for the plant rows. This project’s goal is to develop a machine-vision based, image processing plugin to measure the corn’s population (irrespective of if plant rows are grown in a straight or curvilinear pattern) in the fields and also to count the number of “skips” and “doubles” in the field.

In order to accomplish this goal, the following specific objectives were envisaged: (i) Development of a robust segmentation system to separate plants from the background; (ii) Development of a machine vision algorithm to locate and count the individual plants from the segmented image; and (iii) Determine the distribution of plants along the row in terms of skips and doubles and map the distribution.

3.3. Materials and Methods

3.3.1. Experimental Setting and Image Acquisition

The experiments were conducted at Carrington Research Extension Center (CREC) in Carrington, North Dakota (47°30′29.574″N, 99°7′14.4084″W, elevation 467 m, Google Imagery 2018, CNES/Airbus, Digital Globe, USDA Farm Service Agency). The soil type at the experimental site is a clay. The corn plants have a between row and within-row spacing of 0.6 and 0.3 m, respectively, and the target population was 35,000 per acre. The number of plants within each experimental unit was determined through manual stand counts.

Aerial images were captured from the field using MicaSense RedEdge Multispectral UAV Camera with 6 mm lens mounted on a Hexacopter UAV vehicle (Fig. 3.1) flown at the height of 50 feet above the ground, covering an area of 10 000 m^2 with the 0.05 m ground spatial resolution, when the plants reached V3 to V4 stages. These stages are the vegetative growth stages of corn crop, when the third or fourth leaf collar is visible. This camera has a

capacity of capturing five bands: red band, green band, blue band, NIR band, and RedEdge band. The UAV speed was adjusted initially using the AutoPilot software (software used to fly drones in the MS Windows machine) and the other camera settings were set to default mode. In the field, the wave points were set using the software in order to capture the images. In the CREC laboratory, images were transmitted from the camera to a dedicated computer. The set of captured images were orthomosaicked (uploaded images were stitched using a third-party service online) with the calculated amount of overlapping and then orthorectified with ArcGIS software (ESRI ArcGIS, version) using the set of ground referenced points) and saved as a color tagged image file format (*.TIFF).

Figure 3.1. Hexacopter UAV used in the study.

3.3.2. Plugin Development

Automated plant counting using machine vision involves three major steps. First, the individual images captured by drones need to be stitched together with the applied amount of overlap of the images in order to avoid improper and multiple placements of the objects. Second, the plants must be segmented from the background of soil and other debris. Third, plants must be singulated and counted. The overall algorithm of processing the image for plant-stand count is outlined in the flowchart (Fig. 3.2).

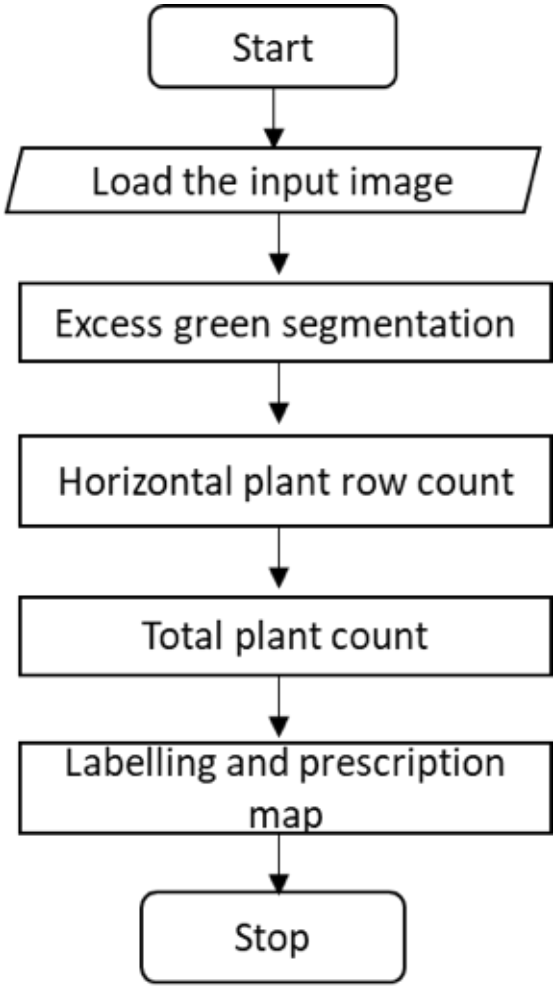

Figure 3.2. Flowchart of the developed plugin to count plant rows and count plants along the rows.

3.3.3. Image Preprocessing

An free and open source Java-based image processing system called ImageJ (`https://imagej.nih.gov/ij/index.html`) is written in Java and allows it to run on Linux, Mac OS X, and Windows, both in 32-bit and 64-bit modes. ImageJ is an open source software and its Java source code are freely available and it resides in the public domain. The integrated development environment used was Fiji (`https://imagej.net/Fiji`), which actually used ImageJ in the backdrop (Fig. 3.3). This system can process different types of images and different size images (8-bit, 16-bit and 32-bit images).

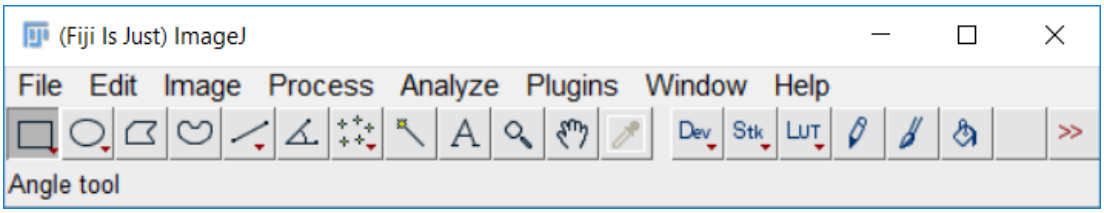

Figure 3.3. Fiji ImageJ integrated development environment.

Fiji was used for the plugin development and the programming environment is shown in (Fig. 3.4). The version used for the plugin development is the ImageJ 1.49b with Java 1.6.0, 64-bit version. In the programming environment (Fig. 3.4), the plugin (user developed program) code is written and compiled to produce the results.

For the plugin the initial development purpose, orthomosaicked stitched image (which was large and represented the whole test plot) were zoomed, cropped and rotated into smaller sections of images (Fig. 3.5). Since the UAV camera captured five different bands of images (R, G, B, NIR, and RedEdge), the plugin was customized so that it can read any type of color or grayscale images (8-Bit, 16-bit, and 32-bit).

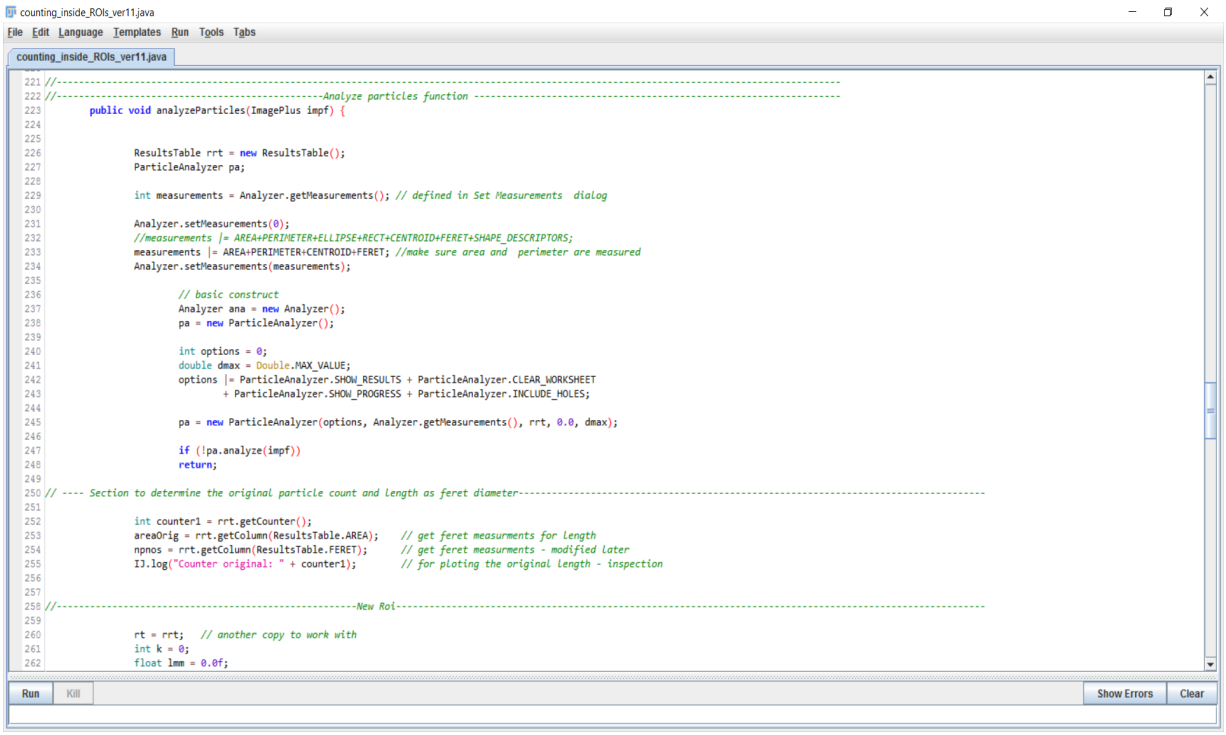

Figure 3.4. Fiji programming environment and plugin development.

3.3.4. Image Segmentation

The initial step in almost in all image processing analysis including the plant population detection is to segment the image by differentiating the pixels into two different classes: main objects in the image (plants) and the background (soil and residues). This step is very important to avoid the misclassification of our desired objects from the image (undesired region). Converting the RGB image into grayscale image did not result in a good division because plant and soil background pixels had similar grayscale values (Tian & Slaughter, 1998). The most common segmentation techniques available for this kind of discrimination are the color index-based segmentation and threshold-based segmentation. Among the color index-based segmentation techniques, though there are several methods available for the segmentation, the well-tested and popular method of ExG color method of

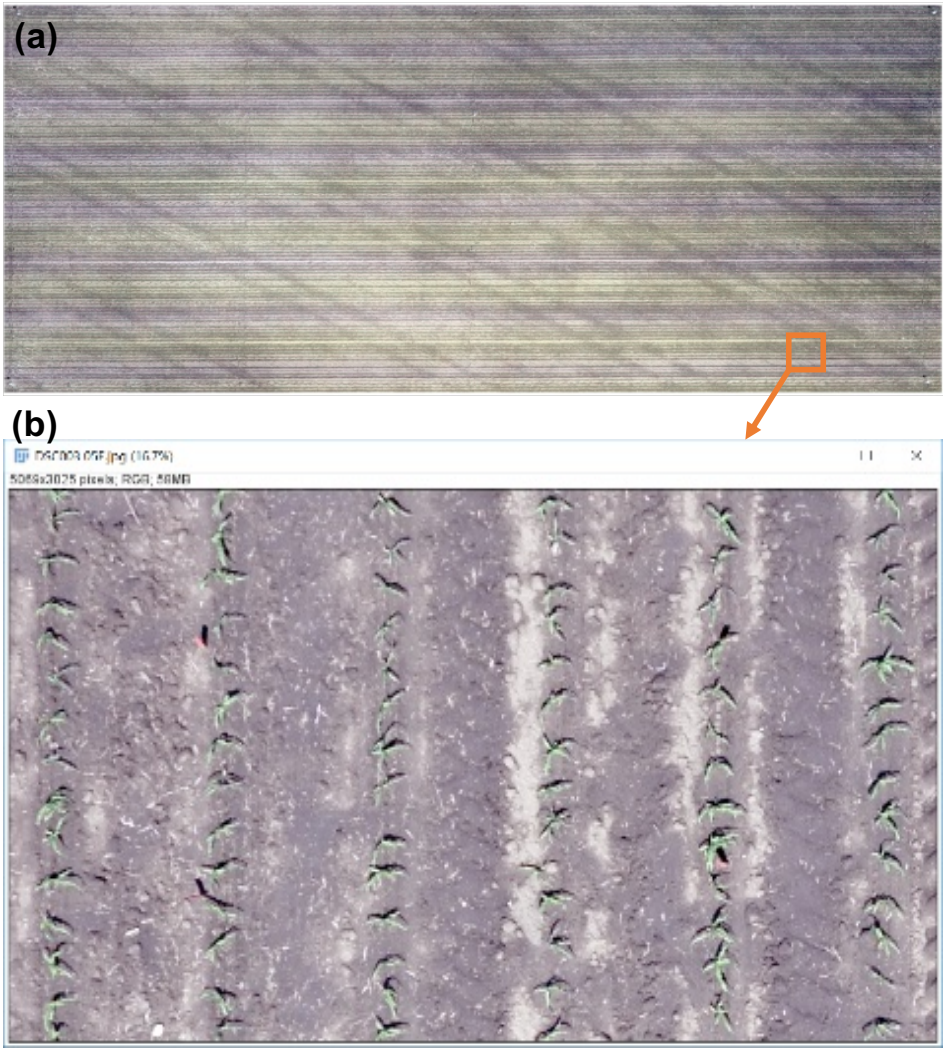

Figure 3.5. Original and input image used in developed plugin. (a) Original stitched UAV image captured at 50 feet and (b) cropped and rotated image that was used as plugin input.

thresholding (Eqs. 2.4–2.6) was selected based on literature (Woebbecke et al., 1995). This method of thresholding was found to provide a clear contrast between plant and soil background (non-plants) from the agricultural field and produced near binary images more precisely than the threshold-based method.

The input RGB image is converted into binary image (segmentation process) using the determined ExG index values (Eq. 2.4) and the user-input threshold value (Eq. 3.1). In

this segmentation process, individual pixel R, G, and B values were read and their ExG were calculated and based on threshold input the pixel will be decided whether it belongs to plant (assigned black) or background (assigned white) using the logic described (Eq. 3.1).

$$\text{Object pixel}_{(x,y)} = \begin{cases} \text{Plant, value} = 0 & \text{ExG} \geq \text{Th} \\ \text{Background, value} = 255 & \text{Otherwise} \end{cases} \tag{3.1}$$

where x, y are the coordinates of the pixel, and 'Th' is the user-input threshold value. The generated segmented image suitable for image processing is presented in Figure 3.6.

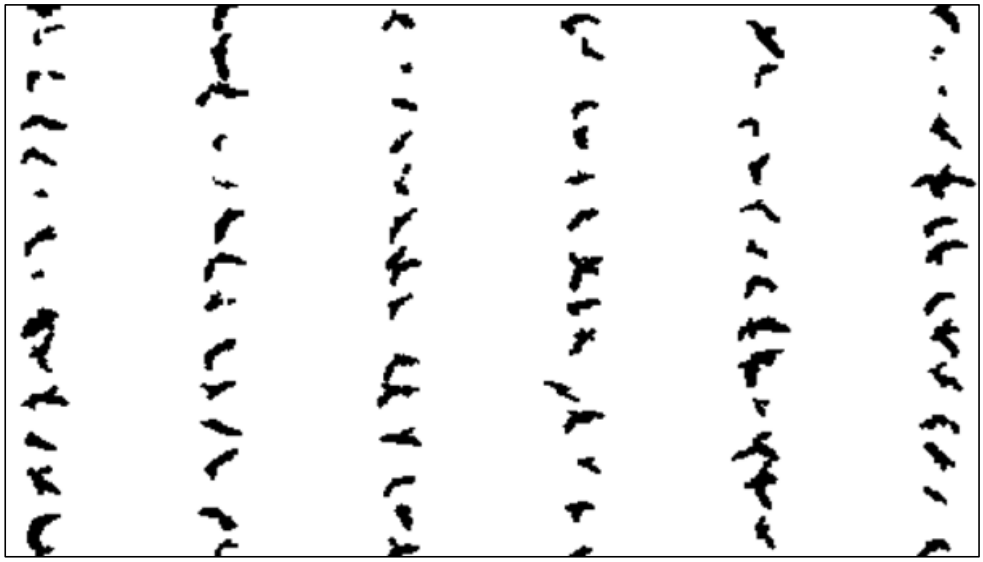

Figure 3.6. Segmented image of rows of corn plants using ExG index.

3.3.4.1. Plugin input panel

To make the plugin interactive, take inputs, and to make the user feel comfortable to use the plugin, the generic dialog box had been added to the plugin as the front input panel (Fig. 3.7). In this front panel, the user provides the inputs, such as the minimum area limit of plants that will remove the small particles in the image (crop residues), the

threshold value for the ExG method, the row, and the plant spacing values. The user also chooses the output options, such as “Particle Analysis” dialog box for making other selections of filtering outputs, display of “Binary image” in the raw form, display of binary image with identified rows, and the display of the final image output of labeled plants. The required images output can be checked or unchecked according to our requirement.

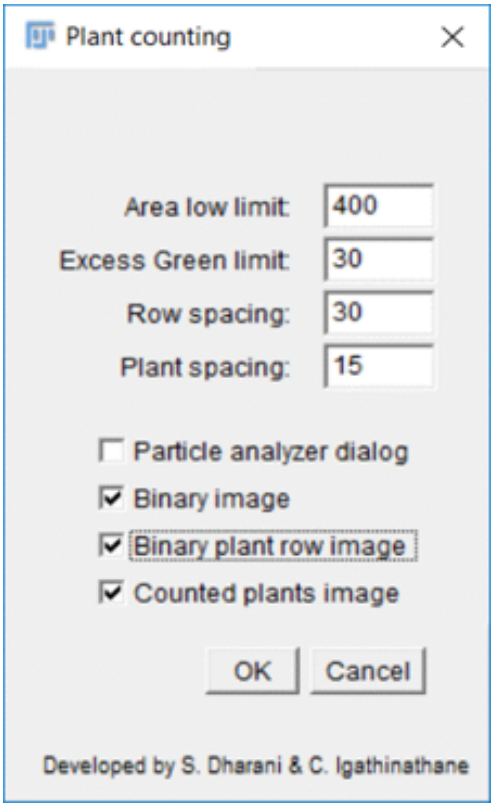

Figure 3.7. Input panel of the plant-stand count plugin.

3.3.4.2. Plant counting using search-hands

After segmentation, the image will be ready to be counted based on a developed “search-hands” method (Fig. 3.8). Search-hands is a new method developed for the plant counting based on white and black pixels in the given image based on “pixel-march” (Igathinathane et al., 2009). In the image, the plant will be the black pixels with the value

of 0, and background will be in white pixels with the value of 255. During pixel-march, the search point moves pixel by pixel based on the chosen direction (any angle will work) and locates the entry and exit of black pixels (belonging to the plants). From the identified black region, the centroid and object profile was obtained and will be used to derive several geometric parameters. From the initial point (lower-left, near the bottom of the first row) the plugin pixel-march will start in the horizontal direction for the first rows in the image to determine the total number of rows in the image. This results will be stored in an array. For each identified row, label numbers will be established. This is called “Horizontal search”.

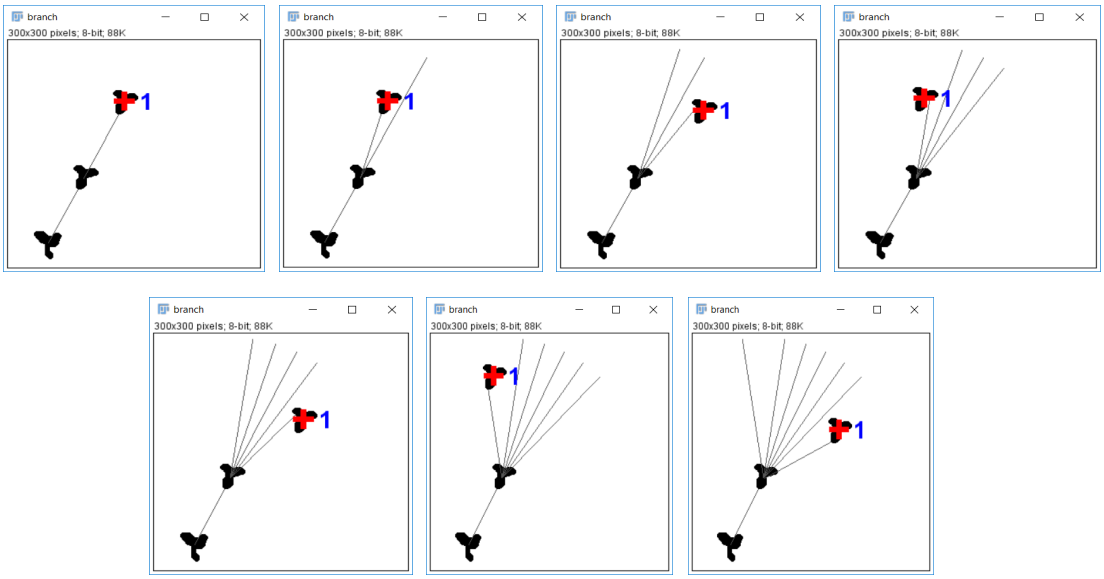

Figure 3.8. Demonstration of search-hands method in seeking out plants that are offset from the row.

After the horizontal search, the counting for each and respective plant row was performed. This is called “Vertical search”. Through this vertical search, each plant in a plant row will be counted and labeled. These searches are done using seven hands. Assuming most of the time the plants are in the center of the row, the center hand will be extended first to count the total number of white and black pixels, which will identify the

plants. If not, first left hand will be extended and then first right hand. If these three hands were not able to identify the plant's pixels, second left and right hand will be extended at a given angle and length, which will be given as an input parameter. Likewise, when the second set of hands were not able to identify the plant pixels, the third set of hands will be extended in the left and right directions (Fig. 3.8).

In the preliminary research, it has been found that three sets of hands (totally six) with a center hand search (predominant in most cases) was sufficient to identify the total number of plant pixels in a given row. The hands were also restricted to an optimal number so that the search hands will not intersect with the neighboring rows. Following this procedure, all the plants of each plant rows were identified.

Once all the image rows were scanned using the plugin and extracted features were recorded. In order to determine the plant counts, the ImageJ's "Analyze Particle" method was used. This command counts and measures objects in binary or thresholded images based on the parameters set with the "Analyze" method using "Set Measurements" commands. This method scans the image or the selected region of interest and then measures several properties of the objects or particles in the image using the "Measure" command. This process gets repeated until it reaches the end of the image or selection. The plant and background regions were further refined using the following rule. Plant areas that were greater than 400 pixel^2, which was fixed based on the image resolution and general plant area, were considered as a required plant region and other plant areas were eliminated. In such a way, the crop residues and other artifacts were eliminated. After this refinement, the plants were counted again and labeled and the regions were refined again through the base rule.

3.3.5. Curvilinear Plant Rows

Sometimes, the straight row crops will not emerge in a straight pattern in the field. Plants are grown in straight or curved patterns based on the field shape or boundary and the planters sow seeds accordingly. In this case, an algorithm counting plants only in the straight pattern will not be sufficient. It should also account for the changes in the plant row pattern, when it is not straight or even deviates a little. The plant's rows may be curved in left or right directions in the field (Fig. 3.9a). The search-hands algorithm, having seven search hands, will account for this curvilinear pattern and capture the plants (Fig. 3.9b). Thus, the algorithm, being robust, captures the plants in any of the patterns such as straight or curvilinear.

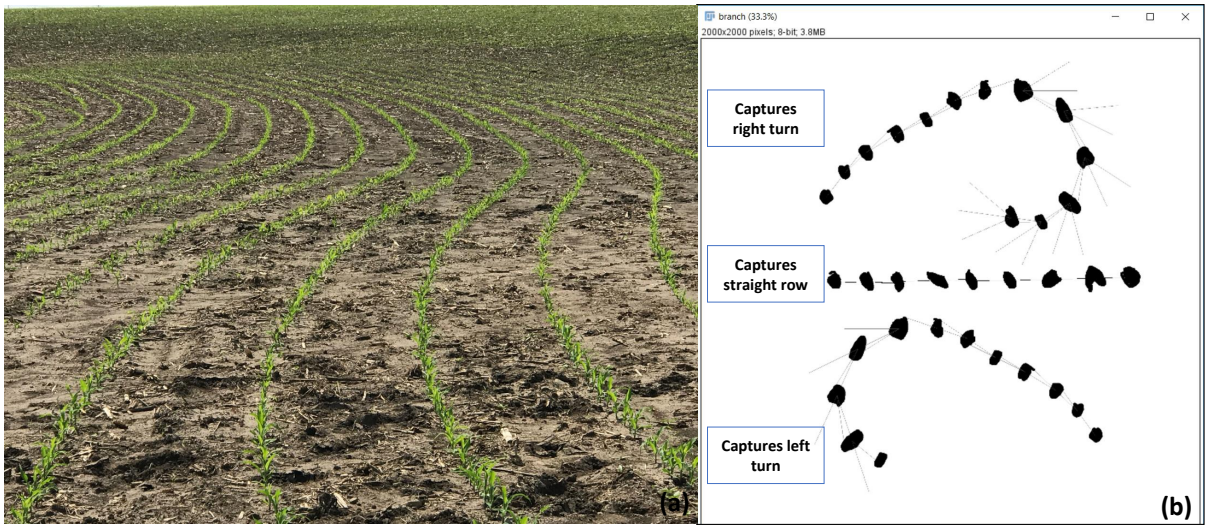

Figure 3.9. Addressing the plant-stand count along curvilinear plant rows (a) Corn crop grown in curvilinear pattern (b) plugin performance in capturing the curvilinear plant rows.

3.3.6. Distance Calculation

After segmentation and plant counting, the distances between the plants were calculated using Feret center X and Y measurements. In order to determine the plant centers, two features were extracted from every row of the binary segmented images: (1) the center position of the plant pixels along each row using Feret diameter measurements. Feret diameter is a measure of the maximum diameter of an object size along a specified direction. In general, it can be defined as the distance between the two parallel planes restricting the object perpendicular to that direction. This plugin gives the output of six ferret measurements: (a) Feret X coordinate of the plant pixel, (b) Feret Y coordinate of the plant pixel, (c) Maximum Feret diameter of the plant, (d) Minimum Feret diameter of the plant, (e) Feret angle of the plant, and (f) center XY positions of the plant pixels. (2) The centroids XY coordinates of the plants. Feret center XY coordinates are calculated using Feret XY coordinates, Feret angle, and Feret diameter, which are the outputs of the standard "Analyze Particles" ImageJ measurements.

Based on centroid XY coordinates too, the distance between the plants could be calculated. However, Feret is a better way of representing the plants using its bounding circle around the plants (Fig. 3.10).

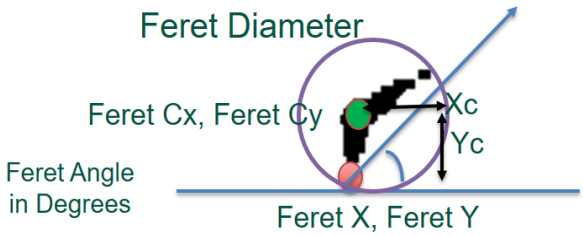

Figure 3.10. Feret Center XY coordinates calculation. Violet circle represents the Feret diameter, red point is the Feret XY coordinates, green point is the Feret Center XY coordinates, and blue lines are showing the Feret angles.

Based on the Feret angle, the Feret center point calculation divided into two cases using the equations Eqs. 3.2–3.5.

$$X_c = (\text{Feret diameter}/2) \times \cos\theta$$

$$Y_c = (\text{Feret diameter}/2) \times \sin\theta$$

$$\text{Feret center}\,X = \text{Feret}\,X + X_c \tag{3.2}$$

Case 1: If Feret angle is Greater than or equal to 90°, then the following calculations are done.

$$\text{Feret center}\,Y = \text{Feret}\,Y + Y_c \tag{3.3}$$

Case 2: If Feret angle is less than 90°, then the following calculations are done.

$$\text{Feret angle} = 180° - \text{Feret angle} \tag{3.4}$$

$$\text{Feret center}\,Y = \text{Feret}\,Y - Y_c \tag{3.5}$$

Finally, plant regions that were more than twice the average distance between the plants were counted as “doubles” and less than the average distances were counted as “skips”. The Feret coordinates were assumed to represent plant center and fall at the middle of the plant region. As the Feret centers generally fall in the plant region, this assumption will not create any undesirable effect while measuring the plant distances.

3.3.7. Labeling the Plants

After counting the plants, they were given the labels based on the count number. The position of the labels was based on the respective centroid and Ferret circle center positions (Fig. 3.11). This will help us to understand the distribution and variability among the plants in the agricultural fields. The "GeneralPath" class from ImageJ was used and this class represents a geometric path with the specified path coordinates. These path coordinates are the Feret center point measurements for the labels to appear on the image (Fig. 3.11).

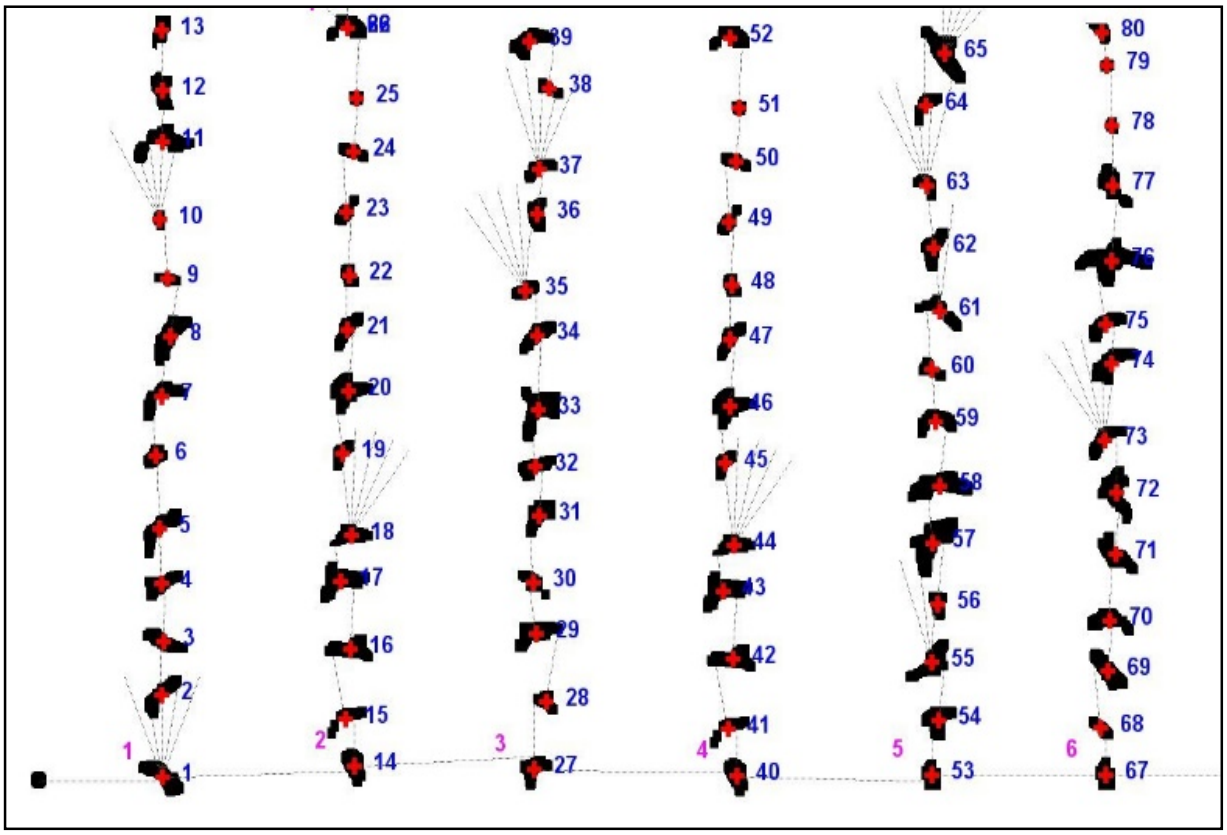

Figure 3.11. Plant-stand count illustration. Plants were labeled and red cross in the image represents the Feret center, blue labels represent the plant count, and pink labels the row count.

First, in the plugin process, horizontal labels are established, which is the total number of plant rows. Then as a next process, for each horizontal row, the total number of plants were counted and labeled.

3.3.8. Results Table

Results table is a table for storing and displaying the measurement results of the plugin (Fig. 3.12). This method had been used to get a reference to the "Results Table" class used by the "Measure" command. The plugin includes 14 measurements of the plants and it is displayed in the tabular form which is useful for the data management. The measurements include parameters, such as Area, Perimeter, Height, width, Angle, Major axis, Minor axis, Centroid XY coordinates, Feret Maximum and Minimum diameter, Feret angle, Feret center XY coordinate of the plants.

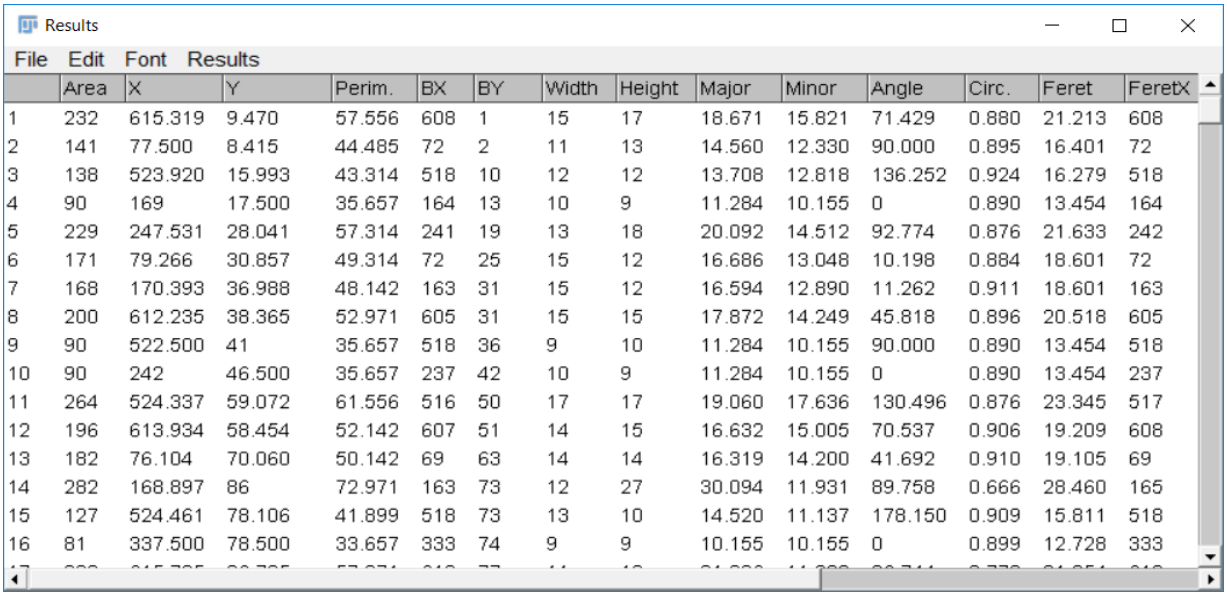

	Area	X	Y	Perim.	BX	BY	Width	Height	Major	Minor	Angle	Circ.	Feret	FeretX
1	232	615.319	9.470	57.556	608	1	15	17	18.671	15.821	71.429	0.880	21.213	608
2	141	77.500	8.415	44.485	72	2	11	13	14.560	12.330	90.000	0.895	16.401	72
3	138	523.920	15.993	43.314	518	10	12	12	13.708	12.818	136.252	0.924	16.279	518
4	90	169	17.500	35.657	164	13	10	9	11.284	10.155	0	0.890	13.454	164
5	229	247.531	28.041	57.314	241	19	13	18	20.092	14.512	92.774	0.876	21.633	242
6	171	79.266	30.857	49.314	72	25	15	12	16.686	13.048	10.198	0.884	18.601	72
7	168	170.393	36.988	48.142	163	31	15	12	16.594	12.890	11.262	0.911	18.601	163
8	200	612.235	38.365	52.971	605	31	15	15	17.872	14.249	45.818	0.896	20.518	605
9	90	522.500	41	35.657	518	36	9	10	11.284	10.155	90.000	0.890	13.454	518
10	90	242	46.500	35.657	237	42	10	9	11.284	10.155	0	0.890	13.454	237
11	264	524.337	59.072	61.556	516	50	17	17	19.060	17.636	130.496	0.876	23.345	517
12	196	613.934	58.454	52.142	607	51	14	15	16.632	15.005	70.537	0.906	19.209	608
13	182	76.104	70.060	50.142	69	63	14	14	16.319	14.200	41.692	0.910	19.105	69
14	282	168.897	86	72.971	163	73	12	27	30.094	11.931	89.758	0.666	28.460	165
15	127	524.461	78.106	41.899	518	73	13	10	14.520	11.137	178.150	0.909	15.811	518
16	81	337.500	78.500	33.657	333	74	9	9	10.155	10.155	0	0.899	12.728	333

Figure 3.12. Results in tabular form using "ResultsTable" class.

3.3.9. Log Output File

The plugin will also give outputs as a log file (default style of ImageJ output) for displaying messages and other information of the plugins (Fig. 3.13). Here several intermediate or final outputs can be generated and the log file will be quite useful while developing the plugin. Any relevant outputs, which may or may not go as rectangular table of values, such as the total number of plants without applying the rule base, total number of plants after applying the rule base, the central processing unit (CPU) taken time to calculate the whole plant counting process, distance between the plants, skips calculation, and doubles calculation can be included in the log output file.

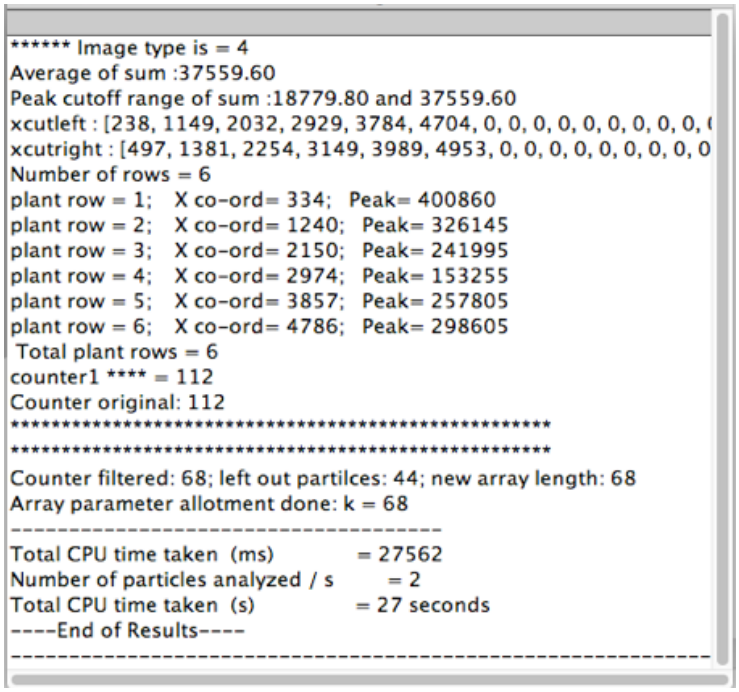

Figure 3.13. Log output file of the plant-stand count plugin.

3.3.10. Message Windows

As a result of running the plugin, the general expectation is to see the final result and a pop-up window is most suitable for the purpose. This was achieved through a

message window where the most relevant results such as the number of plant rows, plant count, skips, and doubles were displayed (Fig. 3.14). This pop-up message windows will be user-friendly for most of the users (mostly farmers/producers).

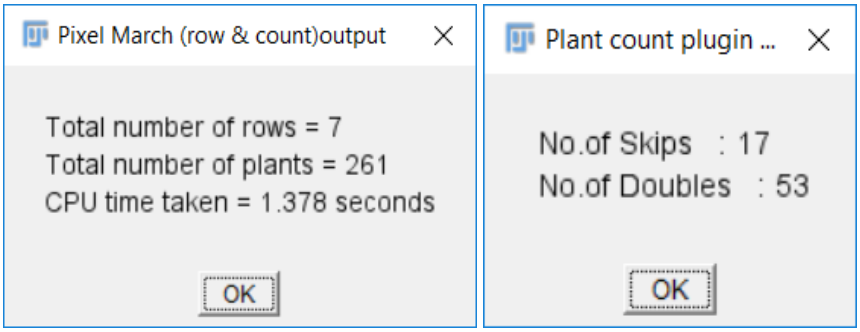

Figure 3.14. Message window output of the major results of the plugin.

3.4. Results and Discussion

3.4.1. Performance of Algorithm with Field Image

The developed plugin was validated using the actual field images. As the field images are larger, for example, one acre image with the drones flight height of 50 ft, some improvisation are required. This image (based on area and resolution) is huge and there is a size limitation in ImageJ. Therefore, to accommodate large images they can be cropped into equal sizes and processed sequentially. Later, for the total count number of plants, the individual results of small sized images will be added to produce the final result. Initial points need to be given as an input to the plugin for the field image. When the plugin was operated with field images as input, the following challenges need to be addressed:

(i) In vertical, slightly distorted from linear, and curvilinear patterns.

(ii) Plants very close to each other.

(iii) Within and beyond the optimum distance.

(iv) Search hands angle — wider or narrower.

(v) Weeds between and within plant rows.

The above-mentioned challenges were considered during the algorithm development to make it as robust as possible to count the plants in the field. Based on the measures, the input search angle for the search hands needs to be adjusted. Wider the angle, the accuracy is decreased as it may skip some plants from total counting and it may interact with the neighboring plant rows which is not correct. Smaller the angle, better it will find the plants that had only a little deviation from the linear. During the development it has been found that 45° is the optimum angle. This could be varied, using trial and error depending on the field image loaded into the plugin. The total number of hands were kept constant as seven, which yielded a good result. Based on the pixel-march method, the search pattern will get adjusted both in the vertical and curvilinear pattern of plants in the field and the search will be completed. A larger image of the plant-stand count of a portion of the field is shown in Figure 3.15.

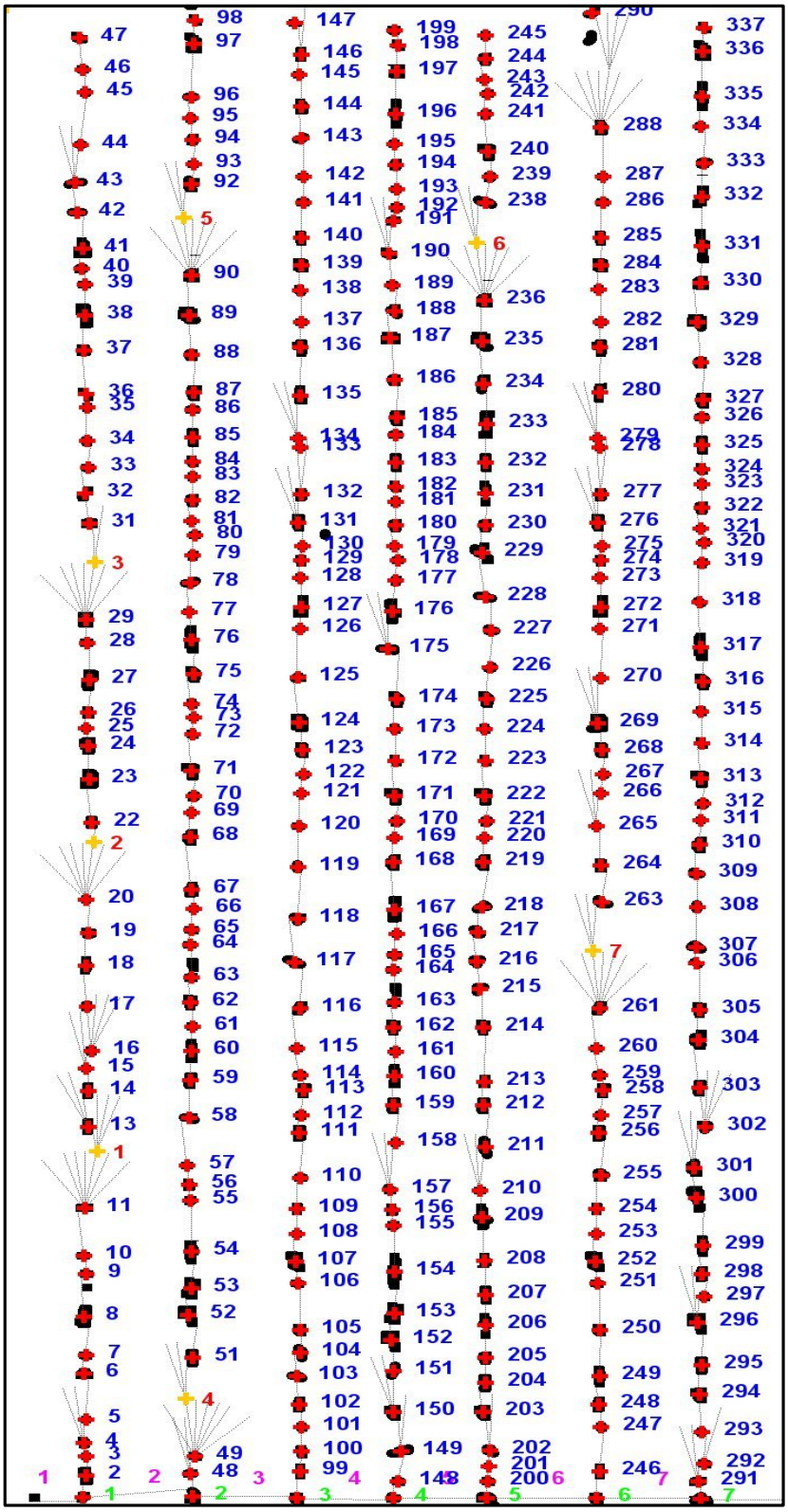

Figure 3.15. Plant-stand count output of a large size field image showing labels.

3.4.2. Field Plant-Stand Distribution Map

To make the plugin output more useful, a plant-stand distribution map is also generated by the plugin (Fig. 3.16). It is a color-coded map of the field that shows the plant population and the spatial plant-stand distribution in the field, such as plants planted and grown at the optimum distance represented in green, above the optimum distance considered as skips represented in red, and below the optimum distance considered as doubles represented in blue. With georeference of any reference points latitude and longitude (e.g., the initial point, any plant, or field corners) along with the field orientation, it is possible to convert this distribution map into a regular map with XY coordinates of the plants to corresponding latitudes and longitudes. The map also serves as an indicator of the seeds germinability and the planters mechanical performance efficiency.

3.4.3. Algorithm Validation

The developed algorithm is versatile to handle any other row type crop field images. Visual counting the plants in the image (usually be zooming-in) is similar to manual inspection in the field. This is termed “Manual count” and that obtained by the program is “Plugin count”, and these were compared in the plugin algorithm and the “Accuracy (%)” was calculated in the validation. The image size with the total number of plants was increased from small to high in the validation. The total number of plants in the images varied from 80 to 500 with a difference of 100 s, tested, and the results are presented along with the computational speed in terms of CPU time (Table 3.1). The algorithm performed irrespective of the size of the field or the number of plants, with an accuracy greater than 99 %. Good segmentation and singulation of objects improve the accuracy of validation.

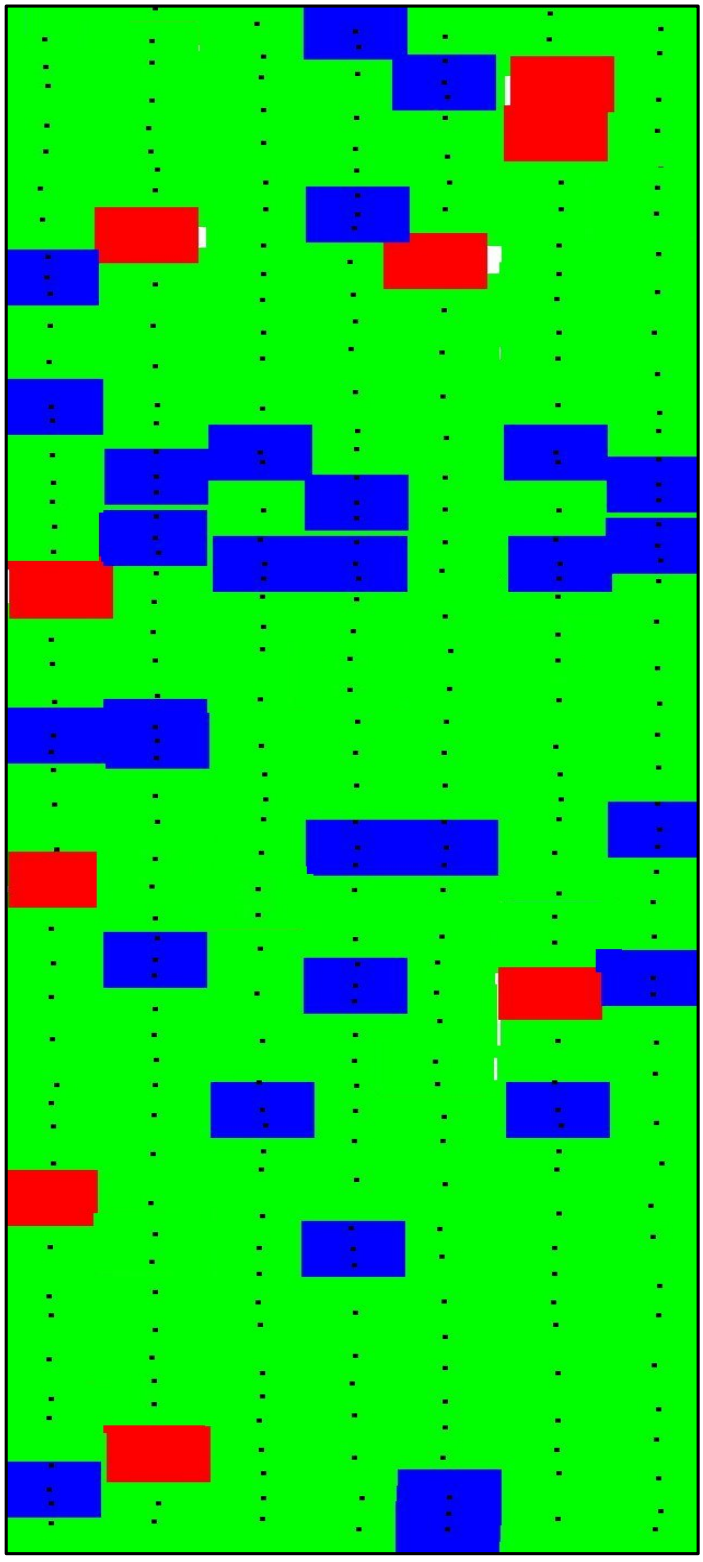

Figure 3.16. Field plant-stand distribution map (Green represents plants under optimum distance, red represents skips and blue represents doubles).

Table 3.1. Plant-stand count plugin validation results.

Validation	Manual count	Plugin count	Accuracy (%)	CPU time taken (s)
# 1	80	80	100	10
# 2	100	100	100	15
# 3	262	261	99.6	17
# 4 (Set 1)	500	496	99.2	20
# 5 (Set 2)	500	497	99.4	25

3.4.4. Limitations and Future Work

One of the main sources of error found was variability in plant size and leaf orientation within an experimental unit. Another issue is the overlap of plants (e.g., well-grown plants touching each other and canopy closing). This made the threshold used to refine the plant and background region sensitive to plant size distribution. Advanced algorithms based on average plant size at different stages and the ideal spacing can be used to resolve the plants touching/overlapping issues. More weed and noise pixels were counted as plants when the area low limit was lowered below 400 pixel^2 and small plants were considered to be weeds when the threshold was increased. However, under low weed conditions and plant growth stage of V3–V4, the system was able to estimate the number of plants along the tested row ($\leq$6.1 m length), and should be tested for other row lengths. The plugin needs to be developed further, for having a web-based interface/plugin to identify the plant rows and to count the total number of plants and their spatial distribution.

3.5. Conclusion

In this study, the pixel-march and search-hand methods were successfully developed using a free, open-source, Java-based ImageJ image processing system, and were tested to

count the plants irrespective of rows' straightness. The skips and doubles included in the analysis, help farmers to predict their yield based on the plant distributions in the fields as well as to evaluate the seed establishment and the planter's mechanical efficiency. The plugin's accuracy was $>99\,\%$, and the calculations took $\leq 25\,\mathrm{s}$ when tested with different plot sizes. The user-friendly message windows with the final plant and row counts, the plant-stand count images with labeled "skips" and "doubles", and the distribution maps to know the precise locations of plants generated by this plugin will be of assistance to producers making field-management decisions.

4. SHAPE-BASED WEED IDENTIFICATION AND MAPPING USING LOW-ALTITUDE UNMANNED AERIAL VEHICLE IMAGES

4.1. Abstract

To achieve sustainable agriculture, there are lots of obstacles, particularly weed management, in today's agriculture. Weeds intervene with the healthy crops' use of resources such as water, spacing, nutrients, and sunlight altering the yield. Recognizing and removing weeds with visual inspection and manual crop scouting are ineffective and tedious for farmers who are managing vast agriculture lands. In this research, a Java-based, ImageJ plugin was developed UAV stitched RGB input images to identify, to locate, and to quantify weeds. Geometrical shape features were utilized to identify and to discriminate between plants and weeds. Six standard shape features from ImageJ were used, and with these features, seven more shape features were derived and incorporated into the algorithm to differentiate crops and weeds. Outputs were produced in the form of a weed-distribution prescription map to visualize the weeds' distribution and location. This algorithm will help farmers to quantify the weeds' infestation level and to determine weed locations in the field in order to deploy site-specific, precise management techniques. This work can be extended to other major row crops in different geographical locations as well as those crops' associated weed identification and quantification.

4.2. Introduction

In order to maintain a better quality and quantity of produce with many crops, applying herbicides is essential. Herbicides account for about 40 % of the total cost for chemical applications, which also include fertilizers, to the field; these chemical applications are done based on the field's total weed infestation (Gianessi, 2005). With modern precision agriculture, site-specific weed management (SSWM) technology is researched and promoted. This strategy is mainly based on customizing herbicide applications at the weeds' location in the field with the applied amount based on the weeds' coverage in the field (Srinivasan, 2006). The SSWM uses spatial data as a major input for the spot application of herbicides in the field.

Most satellite captured images have weed and crop images at the later stages. The optimal time for applying herbicides to control a weed infestation is during the seedlings' early stage. UAVs play a major role in obtaining this spatial information to control weeds in the field. Identifying small weeds in the satellite images is difficult because the satellite captures images at a higher altitude. UAVs can get images by flying at a lower altitude with lots of flexibility, depending on the farmers' field requirements (Torres-Sánchez et al., 2014). This advantage is important to identify weeds during the crop's early stage.
To implement SSWM, it is necessary to have spatial information, such as the weeds' density, location, and type, about the field (Torres-Sánchez et al., 2014).

In SSWM, the eventual objective of identifying the weeds' location and density in the field is to provide a decision-support system for farmers, giving them information, which can be used for herbicide sprayers. To achieve this objective, many algorithms and software programs were developed in order to classify weeds and crops in the fields.

Developing a robust algorithm to identify weed locations during the early crop stage is still challenging. This study addressed this challenge by capturing field images that contained weeds at an early crop stage and weeds for SSWM; this project also developed an algorithm based on object-based methods, thus generating a weed-distribution map for the sprayers to use for placing herbicides at the weeds' exact locations. To achieve this research goal, we developed an image-processing plugin, using a free and open-source ImageJ image-processing system, with two objectives: (i) Identification of weeds by discrimination from crops based on their geometrical shapes, and (ii) Automatic generation of a weed-coverage map from the field image.

4.3. Materials and Methods

4.3.1. Major Weeds in ND

Based on NDSU survey 2017 and other literature, the following weeds were found most predominant in the row crop fields such as corn and wheat. Weeds such as ragweed, lambsquarters, marestail, velvet flower, morning glory were majorly found in the corn field. Among these weeds, two broadleaf weeds lambsquarters and marestail were selected, as these were voted as the most prominent of ND, for the image library development since they are the major competitor for the corn in the field and also which demands more herbicide application.

4.3.2. Algorithm Development

Weed identification using image processing techniques involves three major steps. First, the individual images of crop and weeds such as lambsquarters and marestail were collected and an image library of 45 sub-images for each of the plants considered were developed. Second, the crop and weeds were segmented using excess green segmentation

method. Third, crop and weeds were analyzed based on their geometrical shape features (setting cut-off levels), and weed prescription map was produced. The overall algorithm of identifying and classifying the crop and weeds is outlined in the flowchart Figure 4.1.

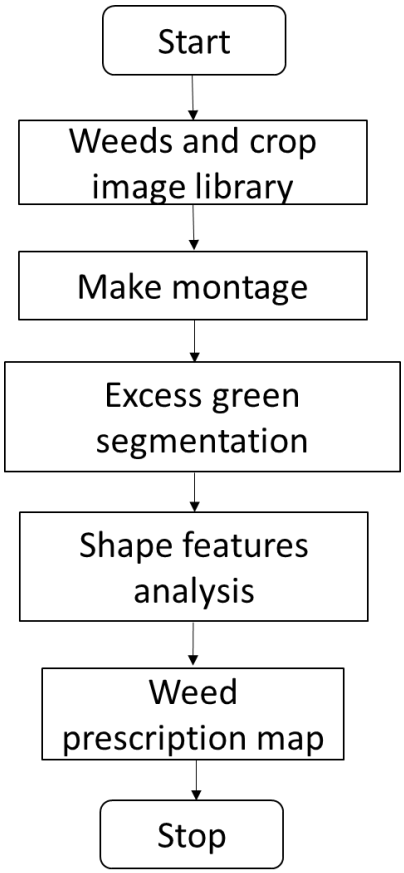

Figure 4.1. Flowchart of the developed plugin to identify and differentiate between corn crop and weeds.

4.3.3. Image Collection and Image Library

Multiple corn images at the V2 stage were collected. Lambsquarters and marestail weeds images were collected from different sources. The weed stage was also similar to corn V2 stage. Images were collected in such a way that different orientations and angles of

weeds and corn crop were considered. Forty-five images of each species (crop and weeds) were collected and an image library was developed for the plugin development (Fig. 4.2).

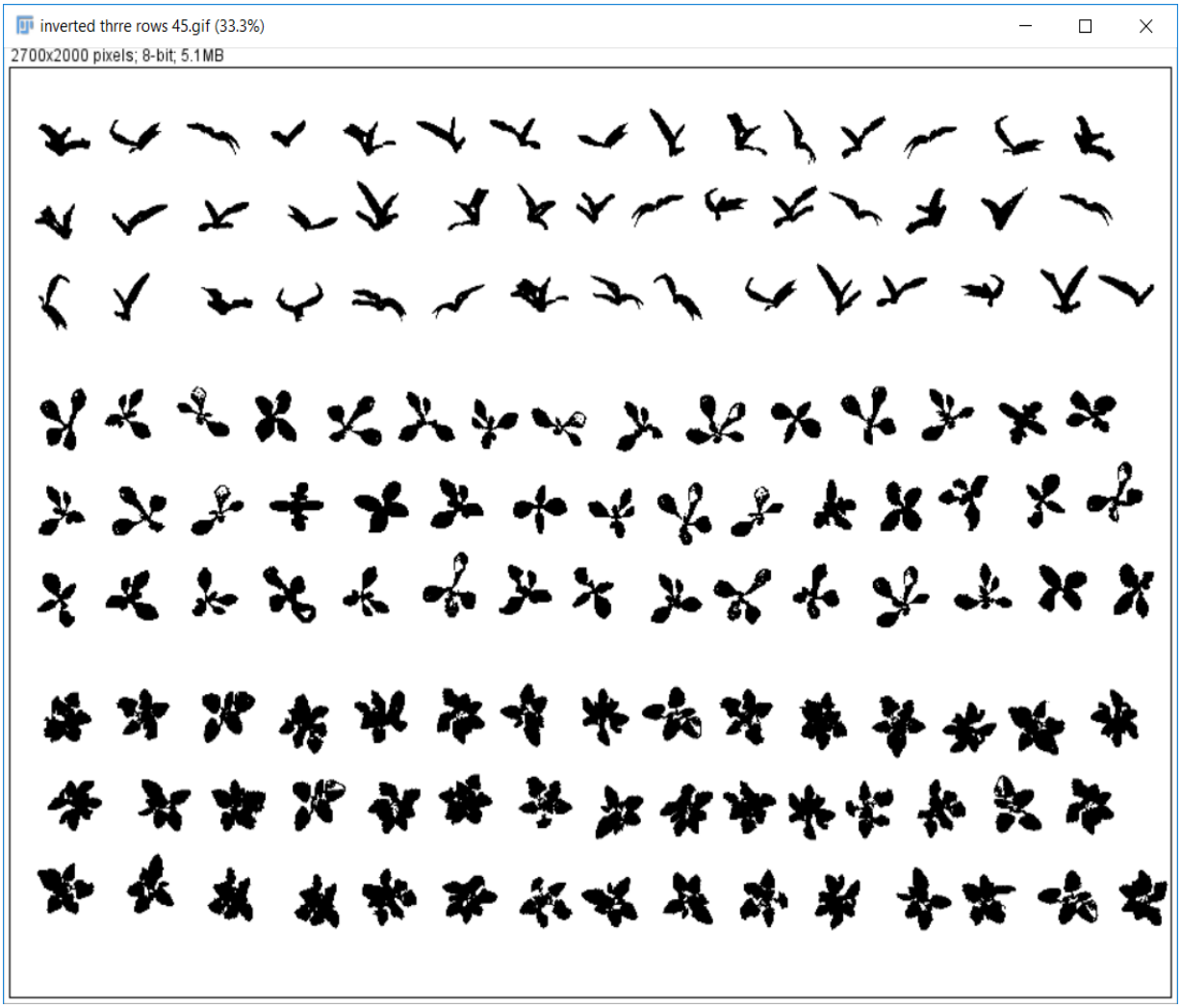

Figure 4.2. Developed image library of corn crop, lambsquarters, and marestail weeds at different angles and orientations.

4.3.4. Image Scaling

Though multiple images were collected from different sources and the images were of different sizes. To make all the images on a uniform size, the images were scaled to a uniform size using image to stack option in ImageJ. Before scaling, the images were

segmented first using ExG segmentation method. After scaling, the montage method was applied to the stacked image set using the ImageJ "Make Montage" dialog box (Fig. 4.3). The montage was done first horizontally until the images were fitted in a row and then a new row was started. This process was continued until all the uniform-sized images were included in the montaged frame were filled.

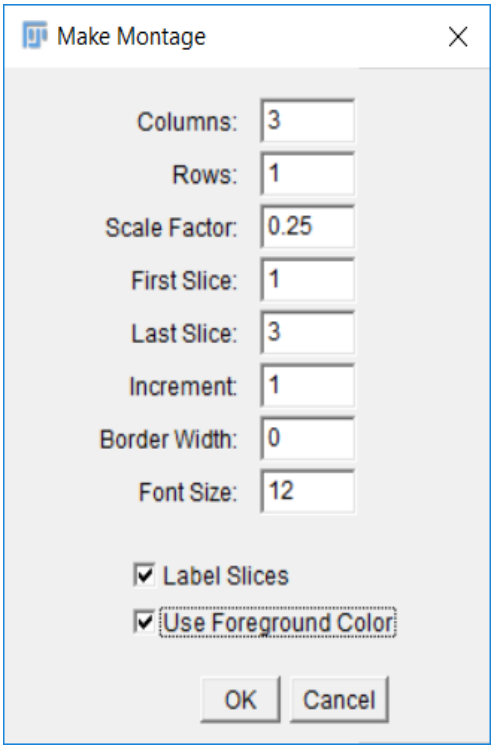

Figure 4.3. Montaging an image stack using Make Montage dialog box.

4.3.5. Geometrical Shape Features

Geometrical features were considered in this study to discriminate the shape between the crop and weeds. Totally, 11 geometrical shape features were considered. Out of 11, four were the standard outputs of ImageJ and seven shape features were derived in the developed algorithm. The four standard ImageJ shape features used in the plugin for crop and weed identification are as follows:

$$\text{Circularity} = \frac{4\pi \times \text{Area}}{\text{Perimeter}^2} \tag{4.1}$$

$$\text{Aspect ratio} = \frac{\text{Major axis}}{\text{Minor axis}} \tag{4.2}$$

$$\text{Roundness} = \frac{4 \times \text{Area}}{\pi \times \text{Major axis}^2} \tag{4.3}$$

$$\text{Solidity} = \frac{\text{Area}}{\text{Convex area}} \tag{4.4}$$

where area and perimeter are the objects area (pixel^2) and perimeter (pixel), respectively obtained from the binary image; major and minor axes correspond to the orthogonal axes (pixel) of fitted ellipse of equivalent area of the object; and the convex area is the area of the convex hull (polygon) that "wraps" the object (pixel^2). All these four features (Eqs. 4.1 –4.4) are dimensionless parameters. Further details on these standard shape features can be found elsewhere (`https://imagej.nih.gov/ij/docs/menus/analyze.html`).

The additional seven shape features derived in this work based on standard ImageJ outputs are as follows:

$$\text{Convex area} = \frac{\text{Area}}{\text{Solidity}}$$

$$\text{Hollowness} = \frac{\text{Convex area - Area}}{\text{Convex area}} \tag{4.5}$$

$$\text{Reverse aspect ratio} = \frac{1}{\text{Aspect ratio}} \tag{4.6}$$

$$\text{Rectangularity} = \frac{\text{Area}}{\text{Bounding rectangle area}} \tag{4.7}$$

$$\text{Feret major axis ratio} = \frac{\text{Feret diameter}}{\text{Major axis}} \tag{4.8}$$

$$\text{Feret minor axis ratio} = \frac{\text{Feret diameter}}{\text{Minor axis}} \tag{4.9}$$

$$\text{Convex area Feret ratio} = \frac{\text{Convex area}}{\text{Feret diameter}} \tag{4.10}$$

$$\text{Compactness} = \frac{\text{Area}}{\text{Feret diameter}} \tag{4.11}$$

where the convex area is obtained from Equation 4.4 (pixel^2), bounding rectangle area is the area of the smallest enclosing rectangle of the object (pixel^2), and the Feret diameter is the maximum diameter of a particle (pixel). Other than the last two (Eqs. 4.10–4.11) shape features, the rest are dimensionless.

4.3.6. Output Message Window

The algorithm calculates the geometrical shape features and outputs the window in a message window (Fig. 4.4). The end users were mostly interested in knowing the final weed density in the field, therefore the algorithm has been designed to display the output separately in the message window along with other forms of outputs (e.g., tables and maps).

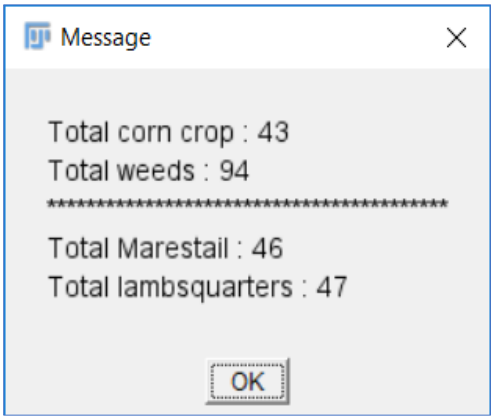

Figure 4.4. Message window with count of total crops and weeds with identified species.

4.4. Results and Discussion

4.4.1. Plugin Shape Features Output

The outputs of the studied standard ImageJ shape features and developed features generated by the plugin are displayed in the tabular form using Results Table (Fig. 4.5). From these tabular form, the main shape feature compactness was found to differentiate between weeds and crops and the compactness value was extracted and given a range in the algorithm to calculate the difference between corn crop and weeds.

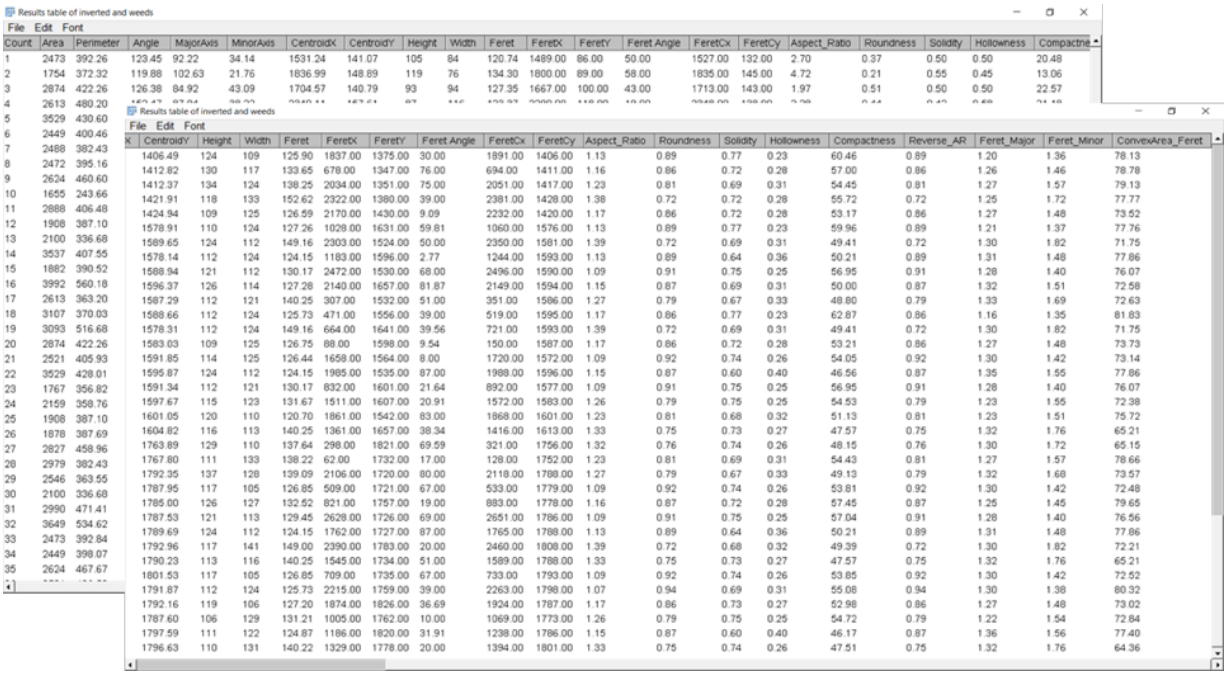

Figure 4.5. Results of standard ImageJ and developed geometrical shape features for crop and weed identification.

4.4.2. Standard Geometrical Shape Features of Weeds and Crops

The shape features from the ImageJ standard outputs (circularity, aspect ratio, roundness, and solidity) did not perform well in discriminating the corn crop and weeds

(Eqs. 4.1–4.11). All of the features were overlapping with each other and it was hard to differentiate between the crop and the weeds (Fig. 4.6).

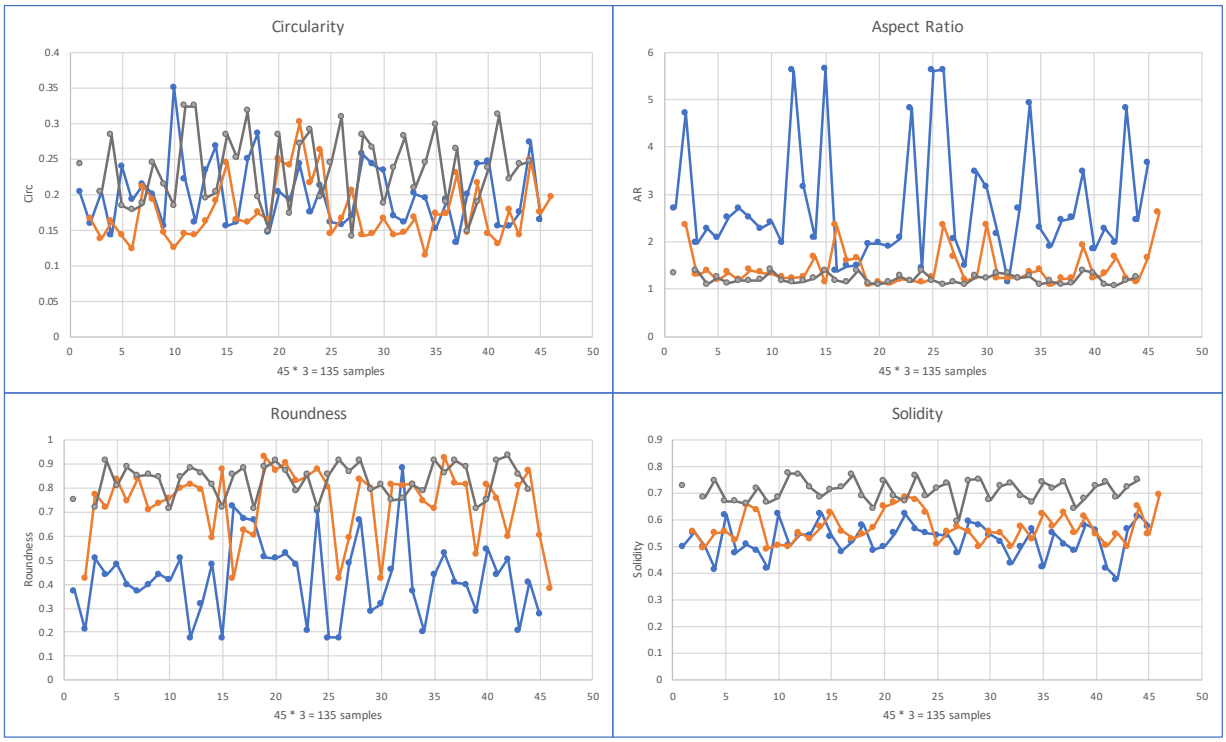

Figure 4.6. ImageJ standard geometrical shape features variation among crop and selected weeds. Blue: corn crop, orange: marestail, and grey: lambsquarters weed.

Among the parameters, circularity ranged from 0.1 to 0.35; aspect ratio ranged from 1 to 6; roundness, which is based on round shape for crops and weeds, ranged from 0.2 to 0.9; and solidity ranged from 0.4 to 0.8; Area of corn crop was approximately 2613 pixel^2. For marestail, it was 5016 pixel^2, and for lambsquarters, it was 6961 pixel^2. Feret diameter for corn crop was approximately on an average 125 pixel^2. For marestail it was 132 pixel^2, and for lambsquarters it was 133 pixel^2. The Feret diameter is almost the same for the corn crop and both weeds. The standard shape features didn't yield good differentiating results. Therefore from these results of standard ImageJ parameters of

circularity, aspect ratio, roundness, and solidity, it has been observed that these shape features because of the observed overlap were not useful in differentiation (Fig. 4.6).

4.4.3. Calculated Geometrical Shape Features of Weeds and Crops

As the standard shape features of ImageJ did not yield good differentiation between the crop and the weeds, the other seven derives shape features were tested. Hollowness ranged from 0.2 to 0.6. The reverse aspect ratio and rectangularity are dimensionless shape parameters varied from 0.2 to 0.9 and 0.2 to 0.6 respectively. Feret major axis ratio varied from 1.2 to 1.8 based on their major axis. These four derived shape features values (Eqs. 4.1–4.4) were again overlapping with each other and they were not useful to discriminate the corn crop and weeds (Fig. 4.7).

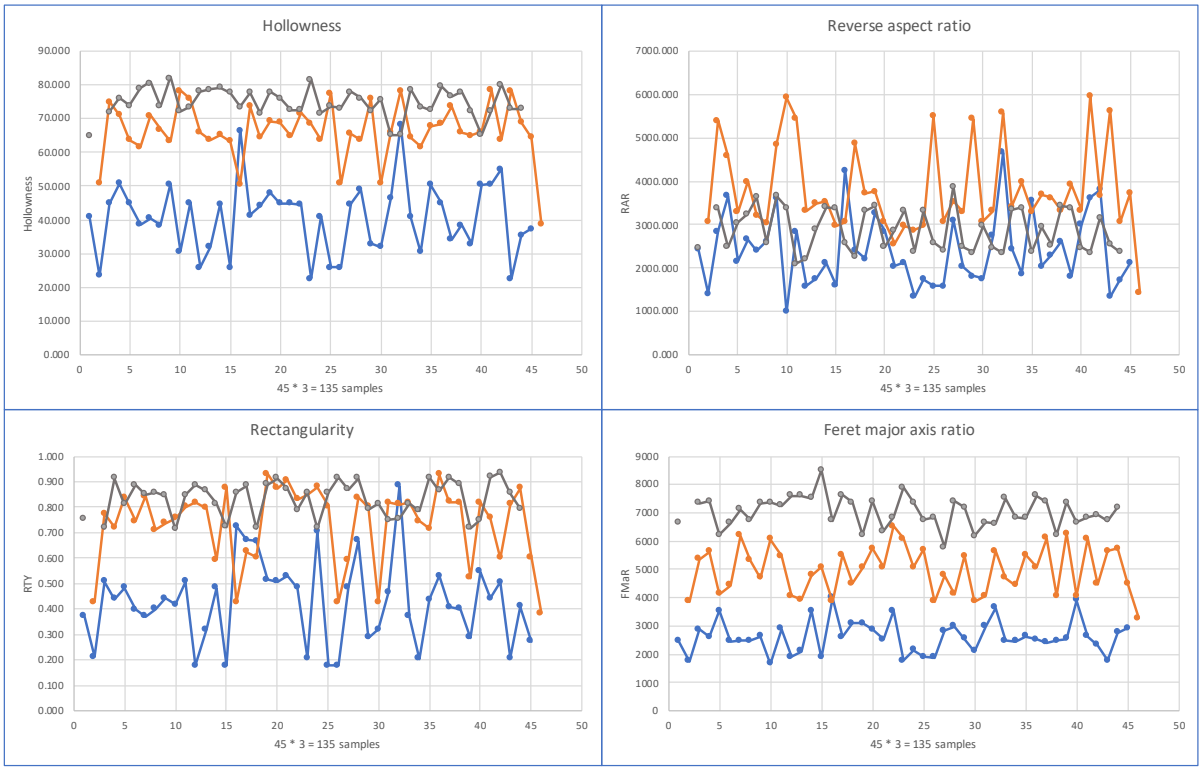

Figure 4.7. Developed geometrical shape features (hollowness, reverse aspect ratio, rectangularity, and Feret major axis ratio) variation among crop and selected weeds. Blue: corn crop, orange: marestail, and grey: lambsquarters weed.

The three other shape features such as compactness, Feret minor axis ratio, and convex area Feret ratio (Eqs. 4.5–4.7) gave good discrimination of various degrees among crops and weeds (Fig. 4.8). Compactness ranged from 10 to 60. Feret minor axis ratio ranged from 1 to 7, and convex area Feret ratio raged from 20 to 85 and the calculated geometrical shape features, Among them, compactness was able to clearly differentiate among corn crop, lambsquarters, and marestail weeds individually from each other with minor overlapping values. Therefore, compactness (Eq. 4.5) was recommended as the best feature for identification of crops and selected weeds.

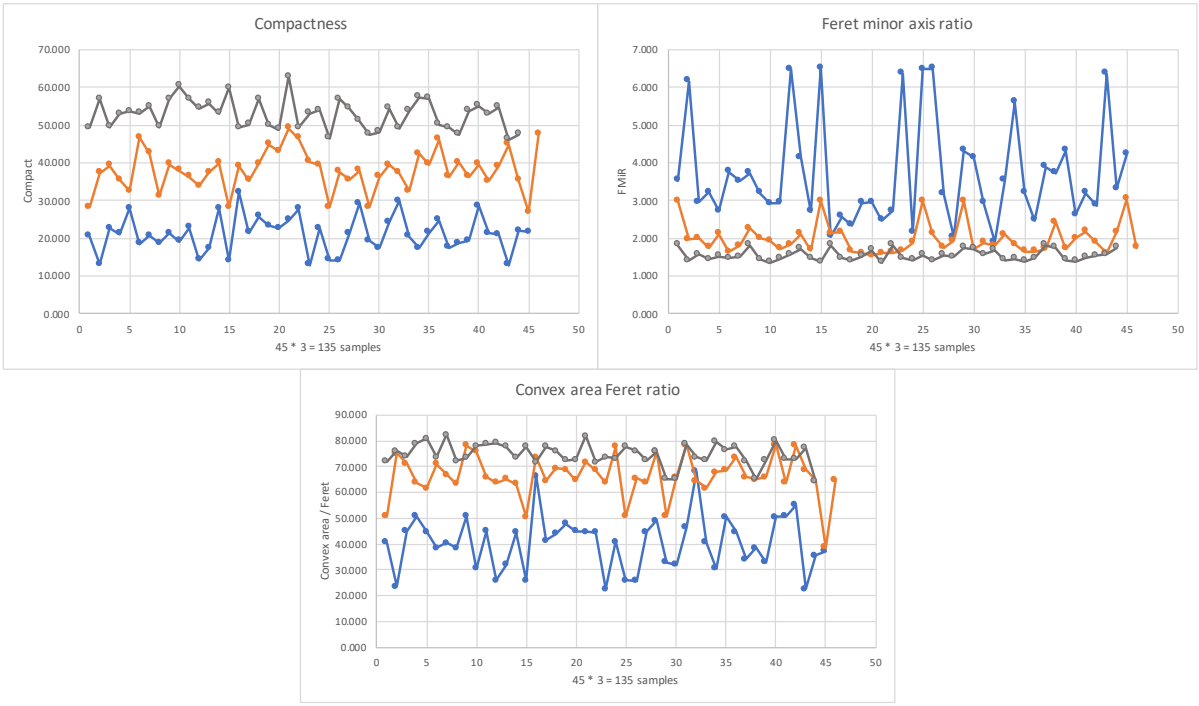

Figure 4.8. Developed geometrical shape features (compactness, Feret minor axis ratio, and convex area Feret ratio) variation among crop and selected weeds. Blue: corn crop, orange: marestail, and grey: lambsquarters weed.

4.4.4. Field Application — Weed Distribution Map

For the autonomous herbicide application process, weed distribution maps were generally used. Production of such maps as one of the outputs of the plugin, to easily

locate the weeds for the herbicide spraying, was included in the algorithm. Weeds located in between the plant rows of a sunflower field infested with marestail were identified and displayed in the form of a weed distribution prescription map (Fig. 4.9). Through this prescription map, the weeds location image coordinates can be calculated and then converted into Universal Transverse Mercator (UTM) coordinates for the spatial application of herbicides. In this way, SSWM will be successfully performed for the precise agriculture applications.

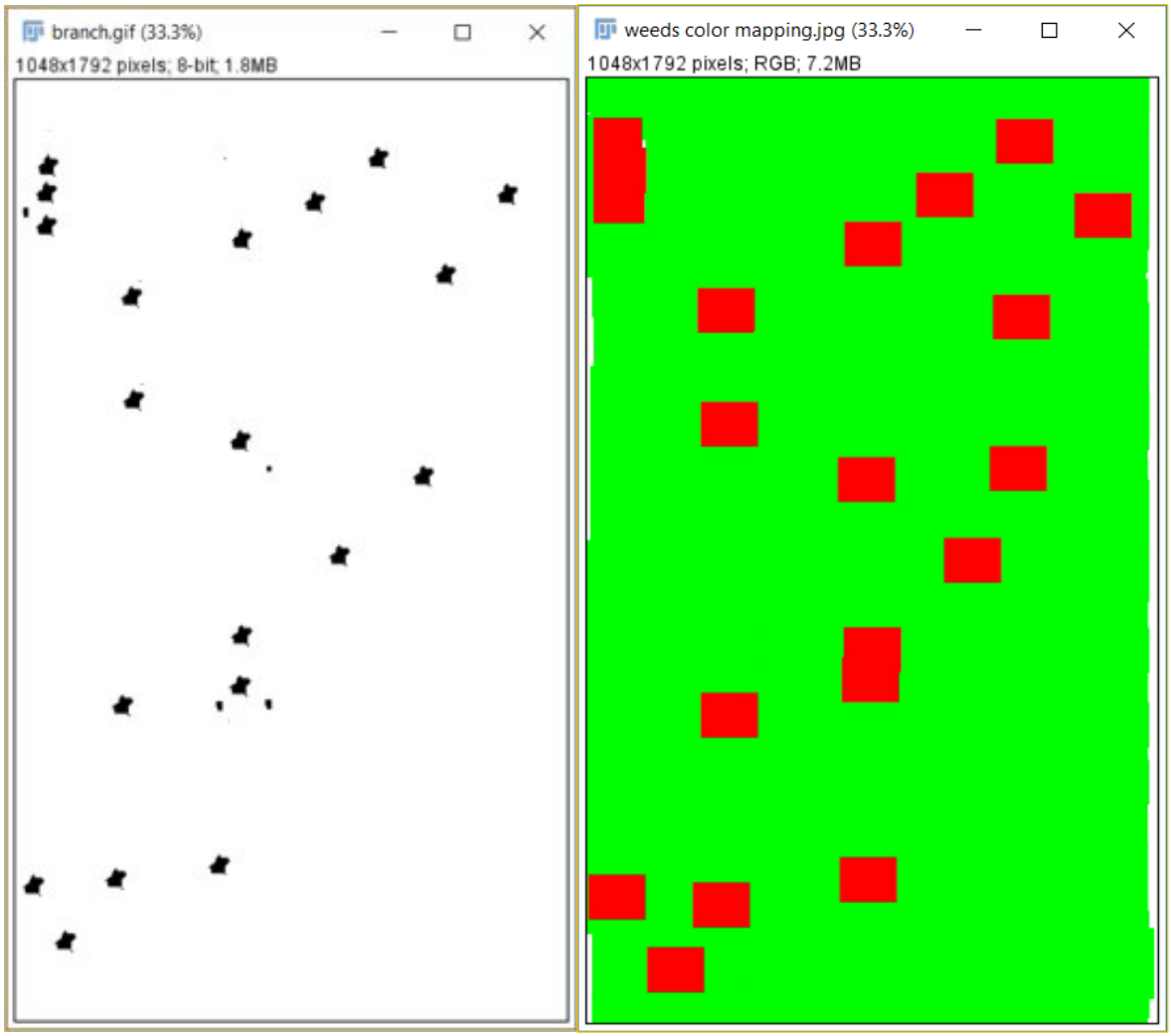

Figure 4.9. Weed distribution prescription map of a sunflower field infested with marestail weeds.

The limits on the selected best discriminating shape features developed from the image libraries could be extended to the field application and this was tested in the sunflower as row crop example with the ragweed as a major weed. The calculated values for lambsquarters were extended to the ragweed and it was found that the algorithm was able to successfully discriminate sunflower crop from ragweed because ragweed and studied marestail had some shape similarity.

4.5. Conclusion

A robust and automated, shape-based image-processing ImageJ plugin program was developed to identify and to map the weed distribution from a developed library of images for corn and weeds of different sizes and orientations. Among the various standard and developed shape features, compactness was the best feature that can clearly differentiate among corn, lambsquarters, and marestail. The algorithm successfully identified the crops and weeds, producing the weed-distribution prescription map. The results were satisfactory and can be used after suitable processing as an input for the sprayers; the georeferenced information gives site-specific, precise spraying locations for herbicides in the field. This will help with the overall estimation of herbicides applied to the field and will help farmers to reduce their input cost and to increase their profit.

5. GENERAL CONCLUSIONS AND SUGGESTIONS FOR FUTURE WORK

5.1. General Conclusions

The UAV applications in agriculture are advantageous by being cost-effective, easily available, efficient, robust, and timely; the applications help farmers/producers to improve their yields by achieving sustainability in agriculture. This technology helps farmers to save time and energy and to increase yield, obtaining more profits than investments. In the future, applying these technologies may reduce human labor and its cost, may increase productivity, and should be given much consideration. In order to utilize this technology, agricultural extension programs should train farmers to fly UAVs in an appropriate way so that people can fully use the technologies' potential. Research related to UAV applications in agriculture by developing software were limited, inspiring the development of this entire research study: reviewing UAVs in agriculture (Paper 1), determining the plant-stand count and distributions in the field (Paper 2), and identifying and mapping weed locations in the field (Paper 3).

A detailed literature analysis was performed, and the highlights of using drones in agriculture were presented. The total number of journal articles that have been published related to work with UAVs in agriculture was presented; this information is useful for researchers to identify the potential areas and research gaps for drone applications in agriculture as well as to develop research studies. In plant-stand counting work, to identify plant distributions in the field, techniques such as ExG segmentation, the pixel-march

method, and the search-hand technique using UAV images were developed and successfully tested in a cornfield. For the weed-identification research, two important weeds in North Dakota, lambsquarters and marestail, both of which are broadleaf weeds, were considered. The geometrical-shape, feature-based analysis (total 11 shape features: standard and derived) was successfully developed to differentiate between the field's crop and weeds, and this analysis determined the weed coverage in a field by producing a weed-distribution map. These outputs help farmers to reduce their input cost for herbicides and to increase their profitability while also being environment friendly.

This research utilized simple and robust image processing techniques to estimate plant distributions and to identify weed locations in the fields, thus not making the process computationally intensive and difficult for the end users to obtain the desired results. The accuracy level for this research was greater than 99% for both plant-stand counting and weed identification. The output was produced in less than 30 s, which is efficient and less time-consuming. This spatial information helps farmers to manage their fields effectively and to be profitable when employing the site-specific precision agriculture. The data help individuals move towards achieving sustainability in agriculture.

5.2. Suggestions for Future Work

There is more scope of future research works in UAV applications in agriculture could be done. Some of the research work possibilities are:

1. Study on plant counting at the later stages of crop growth, when the leaves start overlapping with each other.
2. Extend the study to different row crops as well as identify the various growth stages of the crops.

3. Study on weed identification could be extended by collecting more images and developing the image library with more weeds appropriate to specific locations and needs.
4. Study including different types of images like thermal images, multi-spectral images can be included to identify plant distributions, weed locations, identifying growth stages of plants, which are mainly helpful in crop breeding and physiological studies.
5. Study can be developed based on economics involving from the producers perspective based on grain and biomass yield of the crops.

REFERENCES

Abdullah, N. E., Rahim, A. A., Hashim, H., & Kamal, M. M. (2007). Classification of rubber tree leaf diseases using multilayer perceptron neural network. In *Research and Development, 2007. SCOReD 2007. 5th Student Conference* (pp. 1–6).

Abdullahi, H. S., Mahieddine, F., & Sheriff, R. E. (2015). Technology impact on agricultural productivity: A review of precision agriculture using unmanned aerial vehicles. In *International Conference on Wireless and Satellite Systems* (pp. 388–400).

Aber, J. S., Aber, S. W., Buster, L., Jensen, W. E., & Sleezer, R. L. (2009). Challenge of infrared kite aerial photography: A digital update. *Trans. Kans. Acad. Sci.*, *112*(1/2), 31–39.

Ahmad, I. S., Reid, J. F., Paulsen, M. R., & Sinclair, J. B. (1999). Color classifier for symptomatic soybean seeds using image processing. *Plant Dis*, *83*(4), 320–327.

Aleixos, N., Blasco, J., Navarron, F., & Molto, E. (2002). Multispectral inspection of citrus in real-time using machine vision and digital signal processors. *Comput. Electron. Agric.*, *33*(2), 121–137.

Bullock, D. G., Bullock, D. S., Nafziger, E. D., Doerge, T. A., Paszkiewicz, S. R., Carter, P. R., & Peterson, T. A. (1998). Does variable rate seeding of corn pay? *Agron. J.*, *90*(6), 830–836.

Colwell, R., et al. (1956). Determining the prevalence of certain cereal crop diseases by means of aerial photography. *Hilgardia*, *26*(5), 223–286.

Corbane, C., Jacob, F., Raclot, D., Albergel, J., & Andrieux, P. (2012). Multitemporal analysis of hydrological soil surface characteristics using aerial photos: A case study on a mediterranean vineyard. *Int. J. Appl. Earth Obs. Geoinf.*, *18*, 356–367.

Corkidi, G., Balderas-Ruíz, K., Taboada, B., Serrano-Carreón, L., & Galindo, E. (2006). Assessing mango anthracnose using a new three-dimensional image-analysis technique to quantify lesions on fruit. *Plant Pathol*, *55*(2), 250–257.

Duncan, W. (1958). The relationship between corn population and yield 1. *Agron. J.*, *50*(2), 82–84.

Gianessi, L. P. (2005). Economic and herbicide use impacts of glyphosate-resistant crops. *Pest. Manage. Sci.*, *61*(3), 241–245.

Guerrero, J. M., Pajares, G., Montalvo, M., Romeo, J., & Guijarro, M. (2012). Support vector machines for crop/weeds identification in maize fields. *Expert Syst. Appl.*, *39*(12), 11149–11155.

Guyer, D. E., Miles, G., Schreiber, M., Mitchell, O., & Vanderbilt, V. (1986). Machine vision and image processing for plant identification. *Trans. ASAE*, *29*(6), 1500–1507.

Hague, T., Tillett, N., & Wheeler, H. (2006). Automated crop and weed monitoring in widely spaced cereals. *Precis. Agric.*, *7*(1), 21–32.

Hardin, P. J., & Jensen, R. R. (2011). Small-scale unmanned aerial vehicles in environmental remote sensing: Challenges and opportunities. *GISCI REMOTE SENS*, *48*(1), 99–111.

Honkavaara, E., Saari, H., Kaivosoja, J., Pölönen, I., Hakala, T., Litkey, P., ... Pesonen, L. (2013). Processing and assessment of spectrometric, stereoscopic imagery collected

using a lightweight UAV spectral camera for precision agriculture. *Remote Sens.*, *5*(10), 5006–5039.

Huang, Y., Thomson, S. J., Hoffmann, W. C., Lan, Y., & Fritz, B. K. (2013). Development and prospect of unmanned aerial vehicle technologies for agricultural production management. *Int. J. Agric. Biol. Eng.*, *6*(3), 1–10.

Igathinathane, C., Pordesimo, L., Columbus, E. P., Batchelor, W. D., & Sokhansanj, S. (2009). Sieveless particle size distribution analysis of particulate materials through computer vision. *Comput. Electron. Agric.*, *66*(2), 147–158.

Kataoka, T., Kaneko, T., Okamoto, H., & Hata, S. (2003). Crop growth estimation system using machine vision. In *Advanced Intelligent Mechatronics, 2003. AIM 2003 Proceedings. 2003 IEEE/ASME International Conference* (Vol. 2, pp. b1079–b1083).

Laliberte, A. S., & Rango, A. (2011). Image processing and classification procedures for analysis of sub-decimeter imagery acquired with an unmanned aircraft over arid rangelands. *GISCI Remote Sens.*, *48*(1), 4–23.

Lambert, R., & Faulkner, R. (1991). The efficient use of human energy for micro-scale irrigation. *J. Agric. Eng. Res.*, *48*, 171–183.

Lelong, C. C., Burger, P., Jubelin, G., Roux, B., Labbé, S., & Baret, F. (2008). Assessment of unmanned aerial vehicles imagery for quantitative monitoring of wheat crop in small plots. *Sensors*, *8*(5), 3557–3585.

López-García, F., Andreu-García, G., Blasco, J., Aleixos, N., & Valiente, J.-M. (2010). Automatic detection of skin defects in citrus fruits using a multivariate image analysis approach. *Comput. Electron. Agric.*, *71*(2), 189–197.

Lu, J., Miao, Y., Huang, Y., Shi, W., Hu, X., Wang, X., & Wan, J. (2015). Evaluating an unmanned aerial vehicle-based remote sensing system for estimation of rice nitrogen status. In *Agro-Geoinformatics, 2015, Fourth International Conference* (pp. 198–203).

Mcbratney, A. X., Whelan, B. M., & Shatar, T. M. (2007). Variability and uncertainty in spatial, temporal and spatiotemporal crop-yield and related data. In *Ciba Foundation Symposium 210-Precision Agriculture: Spatial and Temporal Variability of Environmental Quality* (pp. 141–160).

Meyer, G. E., & Neto, J. C. (2008). Verification of color vegetation indices for automated crop imaging applications. *Comput. Electron. Agric.*, *63*(2), 282–293.

Nafziger, E. D. (1996). Effects of missing and two-plant hills on corn grain yield. *J. Prod. Agric.*, *9*(2), 238–240.

Nex, F., & Remondino, F. (2014). UAV for 3D mapping applications: A review. *Appl. Geometics*, *6*(1), 1–15.

Nielsen, R. (2001). Stand establishment variability in corn. AGRY-91-1 (Rev. Nov.-01). Department of Agronomy, Purdue Univ., West Lafayette, IN.

Pena, J. M., Torres-Sánchez, J., de Castro, A. I., Kelly, M., & López-Granados, F. (2013). Weed mapping in early-season maize fields using object-based analysis of unmanned aerial vehicle (UAV) images. *PloS one*, *8*(10), e77151.

Primicerio, J., Di Gennaro, S. F., Fiorillo, E., Genesio, L., Lugato, E., Matese, A., & Vaccari, F. P. (2012). A flexible unmanned aerial vehicle for precision agriculture. *Precis. Agric.*, *13*(4), 517–523.

Quilter, M. C. (1997). *Vegetation monitoring using low-altitude, large-scale imagery from radio-controlled drones* (Unpublished doctoral dissertation). Botany and Range Science Department, Brigham Young University, Provo, Utah.

Rudd, J. D., Roberson, G. T., & Classen, J. J. (2017). Application of satellite, unmanned aircraft system, and ground-based sensor data for precision agriculture: A review. Paper Number: 1700272. In *2017 ASABE Annual International Meeting,* (pp. 1–7).

Sena Jr, D., Pinto, F., Queiroz, D., & Viana, P. (2003). Fall armyworm damaged maize plant identification using digital images. *Biosyst. Eng.*, *85*(4), 449–454.

Shi, Y., Thomasson, J. A., Murray, S. C., Pugh, N. A., Rooney, W. L., Shafian, S., ... others (2016). Unmanned aerial vehicles for high-throughput phenotyping and agronomic research. *PloS one*, *11*(7), e0159781.

Smith, S., & Dickson, S. (1991). Quantification of active vesicular-arbuscular mycorrhizal infection using image analysis and other techniques. *Funct. Plant Biol.*, *18*(6), 637–648.

Srinivasan, A. (2006). *Handbook of precision agriculture: principles and applications*. CRC press.

Stafford, J. V. (2000). Implementing precision agriculture in the 21st century. *J. Agric. Eng. Res.*, *76*(3), 267–275.

Story, D., Kacira, M., Kubota, C., Akoglu, A., & An, L. (2010). Lettuce calcium deficiency detection with machine vision computed plant features in controlled environments. *Comput. Electron. Agric.*, *74*(2), 238–243.

Swain, K. C., Jayasuriya, H. P., & Salokhe, V. M. (2007). Suitability of low-altitude remote sensing images for estimating nitrogen treatment variations in rice cropping for precision agriculture adoption. *J. Appl. Remote Sens.*, *1*(1), 013547.

Tian, L. F., & Slaughter, D. C. (1998). Environmentally adaptive segmentation algorithm for outdoor image segmentation. *Comput. Electron. Agric.*, *21*(3), 153–168.

Torres-Sánchez, J., Peña, J. M., de Castro, A. I., & López-Granados, F. (2014). Multi-temporal mapping of the vegetation fraction in early-season wheat fields using images from uav. *Comput. Electron. Agric.*, *103*, 104–113.

Vericat, D., Brasington, J., Wheaton, J., & Cowie, M. (2009). Accuracy assessment of aerial photographs acquired using lighter-than-air blimps: low-cost tools for mapping river corridors. *River Res. Appl.*, *25*(8), 985–1000.

Warren, G., & Metternicht, G. (2005). Agricultural applications of high-resolution digital multispectral imagery. *Photogramm. Eng. Remote Sens.*, *71*(5), 595–602.

Wich, S., Dellatore, D., Houghton, M., Ardi, R., & Koh, L. P. (2015). A preliminary assessment of using conservation drones for sumatran orang-utan (*Pongo abelii*) distribution and density. *J. Unmanned Veh. Syst.*, *4*(1), 45–52.

Willey, R., & Heath, S. (1969). The quantitative relationships between plant population and crop yield. In *Advances in Agronomy* (Vol. 21, pp. 281–321). Elsevier.

Woebbecke, D. M., Meyer, G. E., Von Bargen, K., & Mortensen, D. (1995). Color indices for weed identification under various soil, residue, and lighting conditions. *Trans ASAE*, *38*(1), 259–269.

Woebbecke, D. M., Meyer, G. E., Von Bargen, K., & Mortensen, D. A. (1993). Plant species identification, size, and enumeration using machine vision techniques on near-binary images. In *Optics in agriculture and forestry* (Vol. 1836, pp. 208–220).

Xiang, H., & Tian, L. (2011). Method for automatic georeferencing aerial remote sensing (RS) images from an unmanned aerial vehicle (UAV) platform. *Biosyst. Eng.*, *108*(2), 104–113.

Zhang, C., & Kovacs, J. M. (2012). The application of small unmanned aerial systems for precision agriculture: A review. *Precis. Agric.*, *13*(6), 693–712.

Zhu, H., Lan, Y., Wu, W., Hoffmann, W. C., Huang, Y., Xue, X., ... Fritz, B. (2010). Development of a PWM precision spraying controller for unmanned aerial vehicles. *J. Bionic Eng.*, *7*(3), 276–283.

Zollinger, R., Christoffers, M., Endres, G., Gramig, G., Howatt, K., Jenks, B., ... Valenti, H. (2006). North Dakota Weed Control Guide. *Fargo, ND, North Dakota State University Extension Service Publication W-253*.

APPENDIX A. COMMON WEEDS OF NORTH DAKOTA

This appendix illustrates the different types of weeds (studied and others) of North Dakota and their identification features.

A.1. Different types of weed identification features

Crops are intentionally planted by farmer and ideally crop should be the only plant in the entire field. Weeds are plants that are not the crop and they may or may not grow in rows. Crops and weeds can be differentiated based on their morphological structure of plants. Differentiating weeds based on its types, growth stages, plant structures like hairs, seed head, growth habit, color, leaf shape, flowers and fruits, and color/shapes is possible. Different weeds, common to North Dakota, and their identification features have been described. Using these features, image processing protocols or algorithms can be developed based on the described weed features such as shape, color, texture, size, and other properties.

A.1.1. Palmer Amaranth

A.1.1.1. Seedlings

Palmer amaranth seedlings have leaves round in shape, pink underside, pink stem, notch on tip of leaves, and are hairless (Fig. A1). This shape and color factor can be considered in image analysis process to identify the early stage plants of palmer amaranth.

A.1.1.2. Mature plants

Mature plants of Palmer amaranth have diamond shaped leaves and petiole is long as leaf (Fig. A1). Sometimes, mature plants have an arrowhead shaped watermark. Stem

grows straight with lots of lateral branches and can be red or green. This weed can grow up to 2 inches/day.

Figure A1. Seedlings and matured stage of Palmer amaranth weed (*Source*: For seedling: `https://aces.nmsu.edu/pubs/_a/A617/welcome.html` and for mature plant: `http://www.mda.state.mn.us/plants/pestmanagement/weedcontrol/noxiouslist/palmeramaranth`).

A.1.2. Water Hemp

A.1.2.1. Seedlings

Water hemp seedlings have pink color underside of leaves and stems (Fig. A2). But this feature to capture in the camera of drone are difficult since underneath of leaves. This could be differentiated by looking at leaves size since water hemp has got leaves longer than palmer amaranth.

A.1.2.2. Mature plants

Water hemp's mature leaves are longer and narrower with shorter petioles, when compared to Palmer amaranth (Fig. A2). Usually, it is difficult to differentiate between

Palmer amaranth and water hemp. However, using the available features, the images can be classified.

Figure A2. Seedlings and matured stage of water hemp weed (*Source*: For seedling: `https://ipm.missouri.edu/IPCM/2010/7/Weed-of-the-Month-Palmer-Amaranth/`, and for mature plant: `https://agrilife.org/coastalbend/program-areas/soil-and-crop-sciences/weeds/weeds-to-watch-out-for/common-waterhemp/`).

A.1.3. Common Ragweed

A.1.3.1. Seedlings

Common ragweed are very common among weed varieties and mostly found in all the agricultural fields(Fig. A3). Common ragweed seedlings have round shape leaves and serrated leaves mostly in even numbers. This can be used as identification feature.

A.1.3.2. Mature plants

Common ragweed mature plants have leaves with multiple lobes and coarse hair with rough texture (Fig. A3). Stems are found to be hairy. This weed can grow up to 8 feet tall. Thus, for image classification, the shape features can be used to identify ragweeds.

Figure A3. Seedlings and matured stage of common ragweed (*Source*: For seedling: https://agfaxweedsolutions.com/2018/04/26/michigan-status-of-herbicide-resistant-weeds-in-2018/, and for mature plant: https://weedid.missouri.edu/weedinfo.cfm?weed_id=17).

A.1.4. Kochia

A.1.4.1. Seedlings

Kochia is another common weed mostly found in the agricultural fields (Fig. A4). Kochia seedlings have long and narrow leaves with hairs giving the leaf a silver tint, which can be used for image identification.

A.1.4.2. Mature plants

Kochia mature plants have lots of branching and they are bushy (Fig. A4). Leaves are lanceolate and have hairs only on margins. Stems are red tint in color. These features are more advantageous and useful for image identification process.

Figure A4. Seedlings and matured stage of kochia weed (*Source*: For seedling: `https://www.gov.mb.ca/agriculture/crops/weeds/print,managing-kochia.html`, and for mature plants: `https://pnwhandbooks.org/weed/problem-weeds/kochia-kochia-scoparia-bassia-scoparia`).

A.1.5. Velvet Leaf

A.1.5.1. Seedlings

Velvet leaf seedlings have leaves in heart shape and has small soft hairs, which can be used for image identification process (Fig. A5).

A.1.5.2. Mature plants

Velvet leaf mature plants have larger heart shaped leave with more dips in the leaf structure with fine soft hairs on stem and leaves (velvet texture) (Fig. A5). Flowers are button shaped. These features helps in identifying this weed variety.

Figure A5. Seedlings and matured stage of velvet leaf weed (*Source*: For seedling and for mature plants: `https://ipm.missouri.edu/IPCM/2015/5/Weed-of-the-Month-Velvetleaf/`).

A.1.6. Morning Glories

A.1.6.1. Seedlings

Morning glory seedlings have cotyledons in butterfly shape and can distinguish between species by looking at differences in shape (Fig. A6).

A.1.6.2. Mature plants

Morning glories mature plants are vine plants climbing on crops and leaves have unique characteristics with purple color flowers, which can be used for image classification process (Fig. A6).

A.1.7. Lambsquarters

A.1.7.1 Seedlings

Lambsquarters seedlings have long narrow cotyledons and small triangular shaped leaves (Fig. A7). Leaves have red outline along leaf margin and stems have silver powder

Figure A6. Seedlings and matured stage of morning glories weed (*Source*: For seedling: `https://oak.ppws.vt.edu/~flessner/weedguide/ipopu.htm`, and for mature plants: `https://www.thriftyfun.com/tf/Gardening/Flowers/Growing-Morning-Glory.html`).

gradient. Triangular shaped leaf features of lambsquarters make them as unique identification feature for image identification process.

A.1.7.2. Mature plants

Lambsquarters mature plants have larger triangular shaped leave with a serrated structure and silvery powder texture on leaves (Fig. A7). Leaves are shaped like a goose foot. These features help in identifying this weed variety.

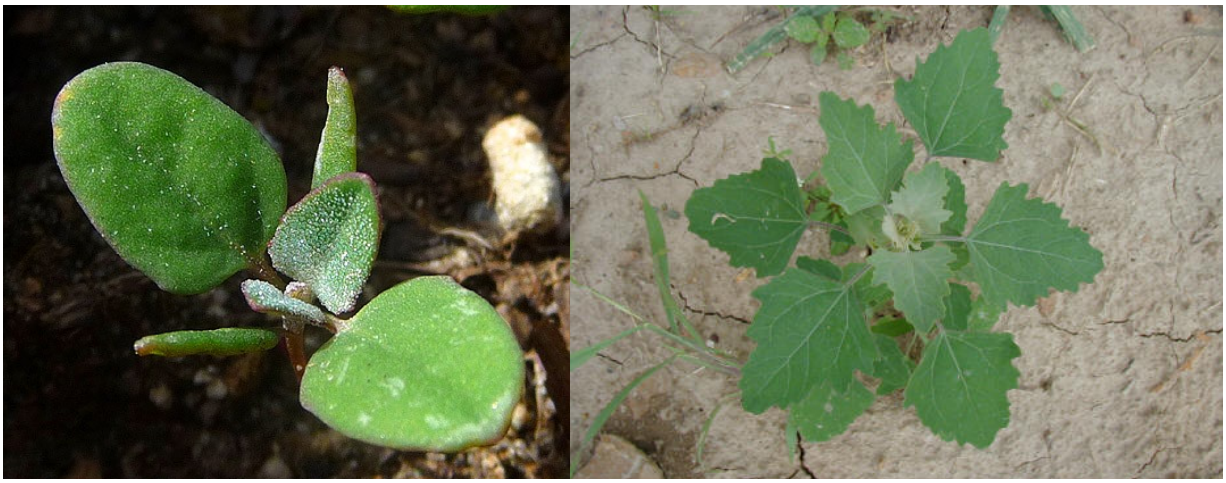

Figure A7. Seedlings and matured stage of lambsquarters weed (*Source*: For seedling: `http://healthyhomegardening.com/Plant.php?pid=285&ss=1536/`, and for mature plants: `https://courses.missouristate.edu/pbtrewatha/common_lambsquarters.htm`).

A.1.8. Marestail

A.1.8.1. Seedlings

Marestail seedlings have leaves with coarse hairs in a rosette shape mostly in a round pattern (Fig. A8). Successive leaves are projected in an apical direction with toothed. Rosette feature is an advantageous feature of marestail, which mainly used as a classification feature for the marestail weed image identification process.

A.1.8.2. Mature plants

Marestail mature plants is an erect herb which can grow up to 1.5 to 6 feet tall with coarse hirsute leaf and stem (Fig. A8). Leaves are grown in a crowded and alternate pattern, which makes the pant to grow in a rosette-like structure. These features helps in identifying this weed variety.

Figure A8. Seedlings and matured stage of marestail weed
(*Source*: For seedling and for mature plants: https://www.no-tillfarmer.com/articles/2309-tips-for-identifying-fall-emerging-weeds/).

APPENDIX B. IMAGEJ CODE - SAMPLES

B.1. Fiji ImageJ System Download Webpage for Different Platforms

Users can download Fiji (Fig. B1), which is a distribution of ImageJ, and includes several plugins and offers a clean color-coded integrated development environment (IDE) for program (plugin) development. ImageJ is a free and open-source image processing system and supports the development of user-coded plugins. The webpage of Fiji for different platforms can be found at `https://imagej.net/Fiji/Downloads`.

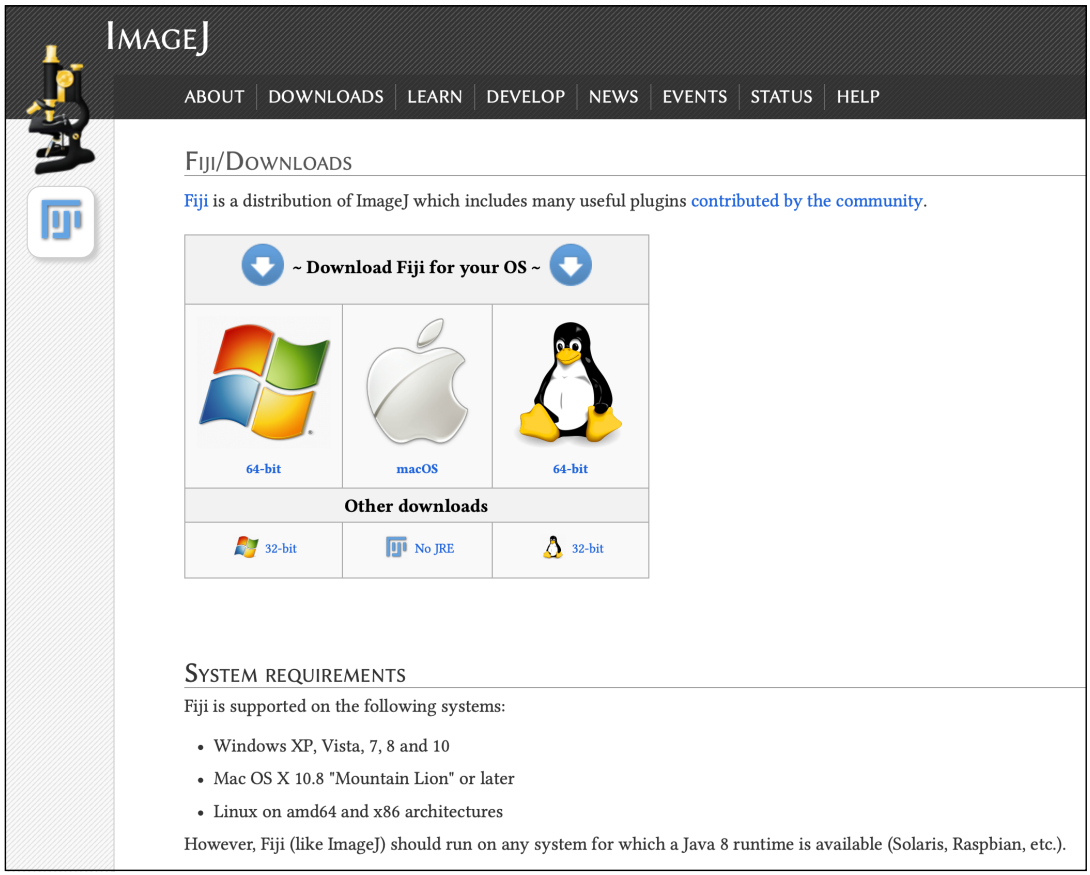

Figure B1. Fiji ImageJ download webpage for different platforms (*Source*: `https://imagej.net/Fiji/Downloads`).

B.2. Sample ImageJ Codes for Plant-Stand Count and Weed Identification

```
// ------------------------------------------------------------
/*
A small portion of original ImageJ code (which is more than 1200 lines for
    plant-stand counting and approximately 500 lines for weed identification) is
    given here. This section contains code for functions like identifying plant
    rows, identifying individual plants and differentiating between weeds and
    plants.
*/
// Developed by: Dharani Suresh Babu and
// C. Igathi; ABEN, NDSU
// ------------------------------------------------------------
// Inputs:
//   ExG                    # Excess Green threshold value
//   xli                    # Initial X1 coordinate
//   yli                    # Initial Y1 coordinate
//   x2i                    # Initial X2 coordinate
//   y2i                    # Initial Y2 coordinate
//   row_plant_spacing      # Spacing between plant rows
//   row_plant_search_angle # Search hand angle search
//   imp                    # Image processor 1
//   imp2                   # Image processor 2
// ------------------------------------------------------------

//###################### Functions ###################

//-----------Excess green segmentation technique --------------

public void do_ExG_binary_mask_and_rows(ImageProcessor ip, int ExGCutoff,
    ImagePlus bimage){

   Image img1; //java.awt.Image

   for (int i=0; i<h; i++) {
         for (int j=0; j<w; j++) {
         PixCol = ip.getPixel(j,i, PixCol);
         R = PixCol[0];
         G = PixCol[1];
         B = PixCol[2];
         ExG = 2*G - R -B;
         if (ExG >= ExGCutoff){
         }  // if
         } // for j
   } // for i
```

```
//-----------------------------------------------------

//------------Identifying plant rows

public int[] Horizontal_initial_branch(int x1, int y1, int x2, int y2, double
    rplant_spacing, double rsang, ImagePlus impin, ImagePlus impout)
{  // ImagePlus is passed

      int [] HNext_branch = new int[3];
      int [] Start_cen = new int[3];

      HNext_branch = hori_Five_points_branching(x1, y1, x2, y2,
          rplant_spacing, rsang, imp, imp2);

      Start_cen[1] = HNext_branch[1];
      Start_cen[2] = HNext_branch[2];

      return Start_cen;
   }
//-----------------------------------------------------

//------------ Efficient Search hand if plant exists or dont exist

public int[] points_branching(int x1, int y1, int x2, int y2, double
    plant_spacing, double sang, ImagePlus impin, ImagePlus impout)
{  // ImagePlus is passed

   if((Plant_found[0]==1 && Plant_found[3] < optimum) ||
       (Plant_found[0]==1 && Plant_found[3] < sec_optimum) ||
       (Plant_found[0]==1 && Plant_found[3] < plant_spacing))
   {// condition check
     //IJ.showMessage("Center line was sufficient");
    //IJ.log("Center points Distance: " + Plant_found[3] );
    }//if

    else{ //if center search fails
         for (int i=0; i<6; i++){  // iterate rest 4 hands
         IJ.log("Slope value: " + m);
         if (m<0){  // slope
                 xp = x[i];
                 yp = y[i];
         }
         else{   //slope
            xp = xf[i];
               yp = yf[i];
```

```
        }

   Plant_found = Pixel_march_two_points(x2, y2, xp, yp, impin, impout);
   return Plant_found;
   }
//-----------------------------------------------------

//--------------- Labeling the plants
public void label_counted_plants(ImagePlus impp, int[]sxsshCen, int[]sysshCen,
    int[]sxssCen, int[]syssCen, int[] sxCen, int[] syCen, int[] skipxCen, int[]
    skipyCen, int stplants, int totplants, int skipplants)

{
   ImageProcessor ip = impp.getProcessor();

   for (int i=0; i < totplants; i++ )
   {//plus symbol for horizontal X and Y centroid coordinates
      path.moveTo(sxssCen[i]-size, syssCen[i]);
      path.lineTo(sxssCen[i]+size, syssCen[i]);
      path.moveTo(sxssCen[i], syssCen[i]-size);
      path.lineTo(sxssCen[i], syssCen[i]+size);
   }

   for (int i=0; i < totplants; i++)
   { //plus symbol for vertical X and Y centroid coordinates
       path.moveTo(sxCen[i]-size, syCen[i]);
       path.lineTo(sxCen[i]+size, syCen[i]);
       path.moveTo(sxCen[i], syCen[i]-size);
       path.lineTo(sxCen[i], syCen[i]+size);
   }

   Overlay overlay = new Overlay();
//-----------------------------------------------------

//------- Weed geometrical shape identification

      for(int i = 0; i < counter1; i++)
      {  //modifying the results table based on max length limits
         lmm = areaOrig[i];
         if (lmm > areaMinLim)
         {
            areas[k] = areast[i];
            per[k] = pert[i];
            angle[k] = anglet[i];
            mAxis[k] = mAxist[i];
            miAxis[k] = miAxist[i];
```

```
      xCen[k] = xCent[i];
      yCen[k] = yCent[i];
      height[k] = heightt[i];
      width[k] = widtht[i];
      feret[k] = ferett[i];
      feretxx[k] = feretx[i];
      feretyy[k] = ferety[i];
      feretangle_xy[k] = feretangle[i];
      circ[k] = circt[i];
      aspectratio[k] = aspectratiot[i];
      roundness[k] = roundnesst[i];
      solidity[k] = solidityt[i];
      compact[k] = areas[k]/feret[k];

if (feretangle_xy[k] <= 90.00)
{
   XFC[k]= (feret[k]/2)*Math.cos(Math.toRadians(feretangle_xy[k]));
   YFC[k]= (feret[k]/2)*Math.sin(Math.toRadians(feretangle_xy[k]));

   feretCx[k]= (int)(feretxx[k] + XFC[k]);
   feretCy[k] = (int)(feretyy[k] - YFC[k]);
}

if (feretangle_xy[k] > 90.00)
{
   feretangle_xy[k] = (int)(180.00 - feretangle_xy[k]);
   XFC[k]= (feret[k]/2)*Math.cos(Math.toRadians(feretangle_xy[k]));
   YFC[k]= (feret[k]/2)*Math.sin(Math.toRadians(feretangle_xy[k]));

   feretCx[k]= (int)(feretxx[k] + XFC[k]);
   feretCy[k] = (int)(feretyy[k] + YFC[k]);
}

CA[k]= areas[k] / solidity[k];
H1[k] = (CA[k]-areas[k])/CA[k];

k++;
   }

}
```